Sonar Tracker Evaluation of Fish Movements Relative To J-Occlusions at The Dalles Dam in 2001

FINAL REPORT

Prepared for:

Battelle, Pacific Northwest Division

P.O. Box 999

Richland, Washington

Prepared by:

John B. Hedgepeth (Tenera Environmental, L.L.C.)

Gary E. Johnson (Battelle Pacific Northwest Division)

Albert E. Giorgi (BioAnalysts, Inc.)

John R. Skalski (University of Washington)

February 15, 2002

EXECUTIVE SUMMARY

The main objective of this study was to compare patterns of fish movement between conditions with and without turbine intake occlusions and J-extensions at The Dalles Dam. (The combination of intake occlusion and J-extension structures is termed a "J-occlusion.") Sampling occurred from April 24 to June 1, 2001. The J-occlusions were moved in and out of the water in 3-day increments according to a randomized block sampling design. Two BioSonics active fish tracking sonars, commonly called sonar trackers, were deployed at Main Unit 1-2. One was mounted on the tip of the J-extension to sample fish movements when the J-occlusions were installed. The other was mounted about 20 m deep on a trashrack to sample fish movements when the J-occlusions were removed from the water. The primary area of interest for both trackers was a region 10 m wide, 15 m from the dam, and 10 m deep, immediately in front of Sluice 1-2. Over 2 million fish positions from about 46,000 fish tracks were obtained during the study. The study entailed three experimental factors: J-occlusions in/out, day/night, and spill/no spill (spill started on May 15).

In general, smolt movements were complex and multi-directional. Fish were not moving through the sample volume in a fixed, consistent direction. Overall, the trend regardless of treatment condition was westward (X-dimension; 56% west out of total west+east) and toward the dam (Y-dimension; 59% toward out of total toward+away). The proportion of fish moving upward in the water column was slightly higher with the J-occlusions in (Z-dimension; 52% up out of total up+down) than out (50%). The proportion of fish moving westward was about the same with (57%) and without (56%) J-occlusions. The proportion of fish moving toward the dam was the same (59%) whether the J-occlusions were in or out. Movements to the west, toward the dam, and upward were 3-5% stronger during day than night. The most dramatic effect on fish movements in front of Sluice 1-2, however, was caused by spill. When water was spilled, the proportion of fish moving westward toward the spillway was 63% compared to 49% during no spill. Also, movement proportions toward the dam and upward were 2-3% higher during spill than no spill. By definition, the zone of influence of the sluiceway was represented by probabilities greater than 0.9 from the Markov-Chain analysis of passage out the sluice side of the sample volume. The sluiceway zone of influence (mean day/night) was larger with the J-occlusions out (40 m^3) than in (22 m^3). In conclusion,

the J-occlusions did not seem to have much effect on fish movements in front of Sluice 1-2, because the J-occlusions did not increase movement proportions up and toward the sluice entrance or enlarge the zone of influence at Sluice 1-2. This implies that if any benefits attend the J-occlusions, they may be associated with decreased turbine passage rates, which this study did not address.

PREFACE

This research was conducted under the auspices of the Corps of Engineers, Pacific Northwest Division's Anadromous Fish Evaluation Program (study code SBE-P-00-017). It is related to and complements surface flow bypass research at other dams and fish passage efficiency (FPE) research at TDA. This broader body of research includes SFB work conducted previously at Bonneville First Powerhouse prototype surface collector (SBE-P-00-6, 8, and 14), Bonneville Second Powerhouse corner collector (SBE-P-00-15), current work on fisheries/hydraulic data integration for Bonneville Dam (SBE-P-0013), Lower Granite prototype removable spillway weir (SBE-W-00-1, 2, 4, and 5), and The Dalles FPE (SPE-P-00-8).

This study was contracted by the Portland District, Corps of Engineers through Battelle Memorial Institute. Battelle subcontracted BioAnalysts, Inc. (Subcontract No. C#407928-BB8), Tenera Environmental (Subcontract No. C#407929-BB8), and BioSonics, Inc. (Subcontract No. C#407927-BB8).

ACKNOWLEDGEMENTS

We are pleased to acknowledge contributions to this study by:

- Battelle Pacific Northwest Division – Russell Moursund, Robert Mueller, Gene Ploskey, Scott Titzler, and Shon Zimmerman
- BioSonics, Inc. – Tim Acker, David Fuhriman, Dale Harkness, Lyle Harkness, Joel Hoffman, Eddie Kudera, Brian McFadden, Colleen Sullivan, Jon Walsh, and Shui Yang
- U.S. Army Corps of Engineers – Steve Dingman, Blaine Ebberts, Dick Harrison, Larry Lawrence, John Nestler, Rich Vaughn, Bill Nagy, and Miro Zyndol

TABLE OF CONTENTS

LIST OF FIGURES

LIST OF TABLES

Section 1: INTRODUCTION

Development of long-term protection measures for juvenile salmon at The Dalles Dam (Figure 1) is a high priority in the endeavor to increase smolt survival through the Federal Columbia River Power System (FCRPS) (National Marine Fisheries Service 2001). The Dalles Dam does not have turbine intake screens, so the only non-turbine passage routes for downstream migrants are the sluiceway and spillway. Estimates of project-wide fish passage efficiency (FPE[1]) range from 80 to 90%, depending on the percentage of spill, among other factors (Ploskey et al. 2001a,b). Thus, there is a need to improve FPE at this critical passage point in the Columbia River.

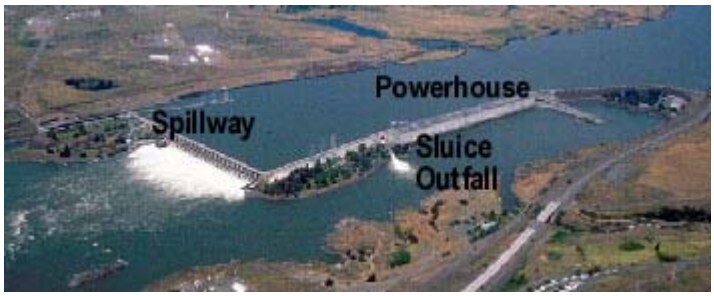

Figure 1. Aerial photograph of The Dalles Dam. Flow is from right to left.

In 2001 at The Dalles Dam (TDA), prototype turbine intake occlusion plates with "J"-extensions[2] were evaluated as a new means of preserving juvenile salmon. The occlusion plates covered the upper half of the intakes at Fish Units 1-2 and Main Units 1-5. When coupled with J-extensions protruding 25 ft from the bottom of each plate, the "J-occlusions" (Figures 2 and 3) caused the turbines to draw water from deeper in the forebay than would otherwise be the case. The premise behind the J-occlusions is that deepening the turbine flow net will decrease entrainment into turbines of juvenile migrants naturally oriented toward the surface. Thus, the intent of the J-occlusions was to decrease turbine entrainment while increasing sluiceway and/or spillway passage, thereby increasing project-wide fish passage efficiency and, ultimately, smolt survival.

[1] FPE is estimated as non-turbine passage divided by total passage.
[2] In this report, we call the combination of occlusion plate and J-extension structures a "J-occlusion."

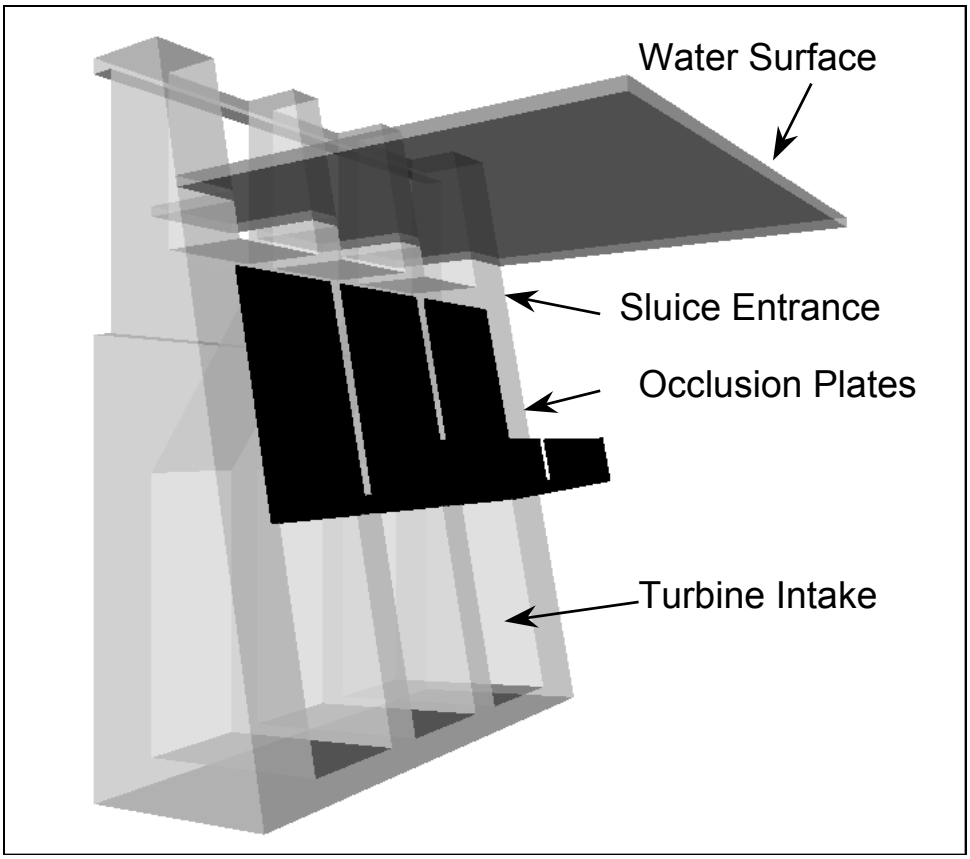

Figure 2. Perspective drawing of TDA Powerhouse Unit 1 showing occlusion plates with J-extensions relative to turbine intakes and sluice entrances.

Before 2001, turbine intake occlusion was tested at The Dalles, Bonneville, Wanapum, and Lower Granite dams with mixed results. In 1995, occlusion plates were first tested at TDA, however, no significant differences in sluiceway efficiency with and without occlusion plates were observed (Nagy and Shutters 1995). In 1996, occlusion plates were evaluated again at TDA, but the results were inconclusive, mainly because of difficulty estimating turbine passage behind the blockages (BioSonics 1996). The 1995 and 1996 tests involved only occlusion plates over the upper portion of the turbine intakes at Main Units 1-5. J-extensions were added for the 2001 test to deepen the turbine flow net. At Bonneville Dam First Powerhouse (B1) in 1996, the upper half of the turbine intakes at Units 3 and 5 were occluded and sluiceway gates at 3B and 5B were opened. The stated purpose of the occlusion at B1 was to intensify and deepen the "zone of separation" between turbine and sluiceway flow nets in an attempt to decrease

turbine passage and increase sluiceway fish passage. Ratios of mean passage rates with and without occlusion plates were 4.8 (with:without) for Sluice Gates 3B and 5B pooled and 0.56 (with:without) for Turbine Intakes 3B and 5B pooled (Ploskey et al. 2001c). However, the differences in passage between conditions with and without occlusions were not statistically significant because daily passage was highly variable (Ploskey et al. 2001c). Based on the results of occlusion plate tests at B1 in 1996, reviewers recommended that turbine intake occlusion be investigated further at dams where enhancing sluiceway passage is a priority (Johnson and Giorgi 1999). At Wanapum Dam, the surface attraction channel that was installed on the forebay side of the powerhouse essentially occluded the upper 20% of the turbine intakes. The apparent effect was to reduce turbine entrainment rates at intakes below the channel (Kumagai et al. 1996). At Lower Granite Dam in 1998, a Simulated Wells Intake (SWI) was retrofit on the existing surface bypass and collector structure. The SWI occluded the upper 20% of the intakes at Units 4-6. A fish budget analysis of juvenile passage from hydroacoustic data indicated that the SWI reduced turbine entrainment when the fish budget coefficients were compared to previous studies without the SWI (Dauble et al. 1999). Thus, the collective results of occlusion plate tests were promising enough that, in conjunction with deepening of the turbine flow net from the new J-extensions, research on the J-occlusions at TDA was a high priority in 2001.

As part of the overall J-occlusion evaluation effort, we collected data on smolt movements in front of Sluice 1-2 from April 24 to June 1, 2001. Other researchers used radio telemetry and hydroacoustic techniques to assess the performance of the J-occlusions, i.e., estimate FPE, spillway and sluiceway efficiencies, and spill, sluice, and turbine passage rates. The sonar tracker data will be useful to interpret and explain the J-occlusion performance data, which will be the “bottom-line” for decisions about the J-occlusions.

The objectives of the sonar tracker study were to:

1. Describe smolt movements patterns in terms of observed fish velocities, streamtraces, and fates[3].

2. Compare smolt movement patterns with and without J-occlusions in place.

[3] Fates are probabilities on which side a tracked fish will exit the sample volume.

3. Assess specific hypotheses about smolt movements, including:

   - the zone of influence of the sluiceway as determined by fate probabilities will be larger with J-occlusions than without;
   - the overall probability of passage toward the turbines will be lower with J-occlusions than without;
   - the overall probability of passage toward the west will be higher with J-occlusions than without.

This report is organized with the introduction in Section 1, followed by a study site description in Section 2. The methods and results are presented in Sections 3 and 4, respectively. The discussion is contained in Section 5. The main body of the report closes with conclusions and recommendations in Section 6 and literature cited in Section 7. Appendix A provides technical data on the active fish tracking sonar. Appendix B provides a description of some of the methodology and processes involved in tracking mechanics.

Section 2: STUDY SITE DESCRIPTION

General

The Dalles Dam, located at river kilometer 308, is the second closest dam in the FCRPS to the Pacific Ocean. It has a 637 m long powerhouse with a total generating capacity of 1,814 MW. Total hydraulic capacity of the 22 unit powerhouse is about 10,619 m^3/s (375 kcfs). Full pool elevation is rated at 48.7 m (160 ft) above mean sea level. Minimum operating pool elevation is 47.2 m (155 ft). The sill at each sluiceway entrance is at elevation 46.0 m (151 ft). The turbine intake ceiling intersects the trashracks at elevation 43.0 m (141 ft). The face of the dam is at an 11.3° angle off vertical (Figure 3). The 421 m long spillway is comprised of 23 bays with Tainter gates. A bathymetric map of the forebay shows the main channel of the river along the south shore, and deep areas in front of the powerhouse (Figure 4). Much of the forebay, however, is relatively shallow (< 20 m deep).

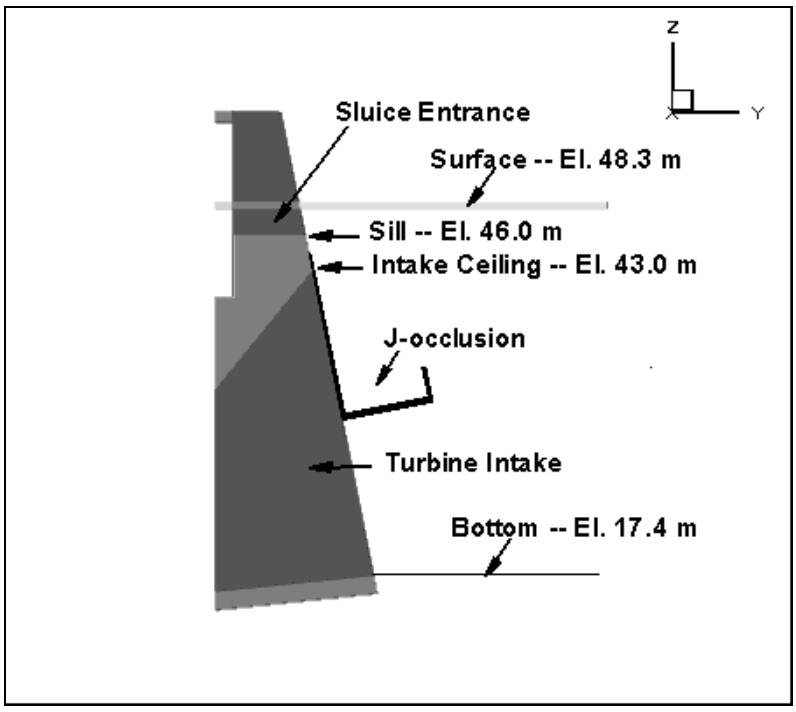

Figure 3. Sectional view of The Dalles Dam powerhouse showing sluiceway entrance, sill, turbine intake, and J-occlusion.

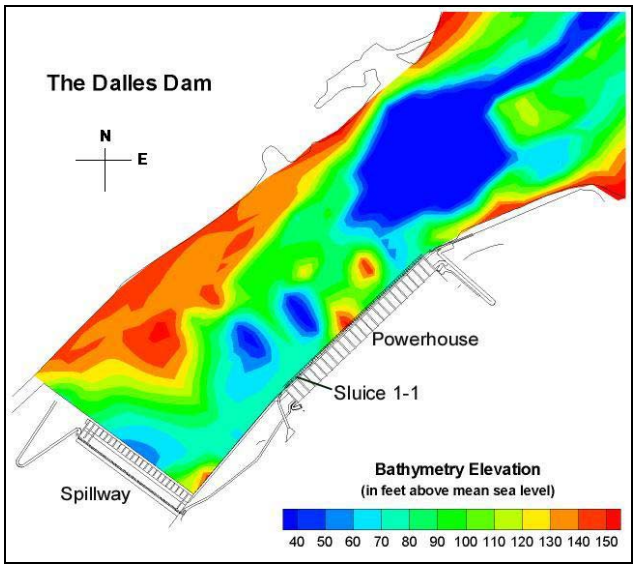

Figure 4. Plan view of The Dalles Dam showing forebay bathymetry.

Sluiceway

The ice and trash sluiceway at TDA extends the entire length of the powerhouse. During the fish passage season (April through November), the three gates at Main Unit 1 are typically opened. This operation is based on previous research (e.g., Nichols and Ransom 1980). The capacity of the sluiceway is limited hydraulically to about 135 m^3/s to 142 m^3/s (4,750 to 5,000 cfs) because of a constriction in the downstream end of the channel near where it exits the powerhouse. Water enters the sluiceway from the forebay when automatic hoists move leaf gates off a sill at elevation 46 m (151 ft). Sluiceway discharge is a relatively small proportion of total project discharge (~1-5%).

J-Occlusions

The J-occlusion plates are panels that can be lowered in front of the existing trashracks, thereby blocking or preventing flow from entering the turbine intake above an approximate elevation of 100 ft. Various shapes of blocked trashracks were studied in physical models at ERDC (ENSR 2001). A J-shaped blocked trashrack appeared to be the most effective in creating flow conditions favorable for collection of juvenile fish in the ice and trash sluiceway. Figures 2 and 3 show gross details of the J-shaped blocked

trashrack. The J-extension of the blocked trashrack consists of 25- and 10-foot panels, 24 ft wide. The J-occlusions were raised and lowered with winches.

River Environment and Project Operations

During our study (April 24 to June 1, 2001), river discharge at TDA ranged from 2,613 to 4,796 m^3/s (92.3 to 169.4 kcfs) (Figure 5). Mean daily discharge was 3,738 m^3/s (132 kcfs). Discharge peaked in late April and declined throughout the remainder of the study. Average discharge from January through July 2001 at TDA was 57% of that in 2000. Daily powerhouse discharge during the study averaged 3,225 m^3/s (113.9 kcfs). Spill for fish protection in the "juvenile pattern" was not commenced until May 15 when 30% of total discharge was released, day and night. Daily spill flow during our study varied from 0 to 1,501 m^3/s (0 to 53 kcfs), with a mean of 513 m^3/s (18.1 kcfs) (Figure 5).

Forebay elevation during the study ranged from 48.0 to 48.6 m (157.6 to 159.5 ft) (Figure 6). Mean forebay elevation was 48.4 m (158.9 ft). With Gates 1-1, 1-2, and 1-3 fully open and the forebay at elevation 158 ft, sluice discharge is 3,800 cfs (rating curve provided by Chris Goodell, Corps of Engineers Portland District, pers. comm.). Thus, sluice discharge was about 2.9% of mean daily discharge for the total project and 3.3% of total powerhouse discharge.

Water temperature during the study generally increased from 9.8 to 16.9° C (Figure 7). Turbidity was generally low, averaging 4.2 NTU (Figure 7).

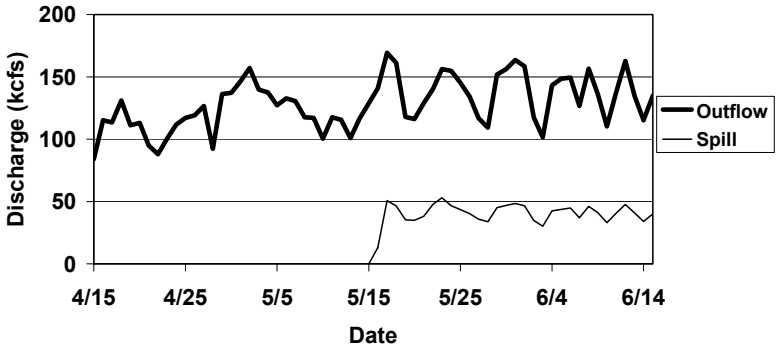

Figure 5. Total outflow and spill (kcfs) from 15 April – 15 June 2001 at TDA. Data were obtained from DART, an Internet website (http://www.cqs.Washington.edu/DART/).

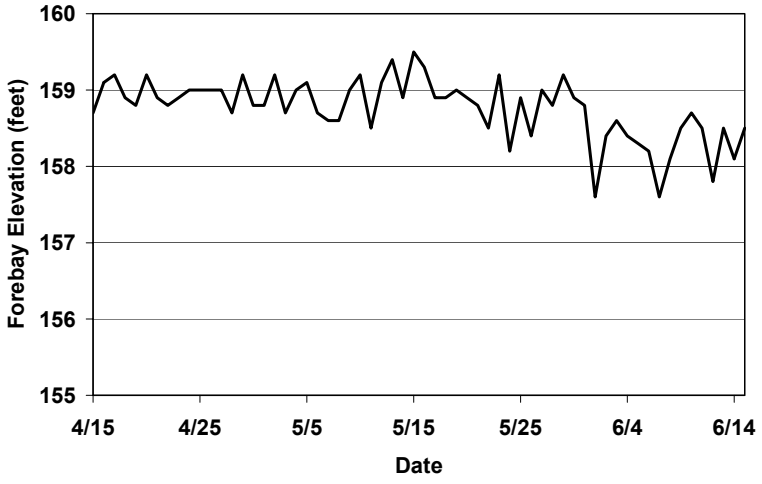

Figure 6. Forebay elevation from 15 April – 15 June 2001 at TDA. Data were obtained from DART, an Internet website (http://www.cqs.Washington.edu/DART/).

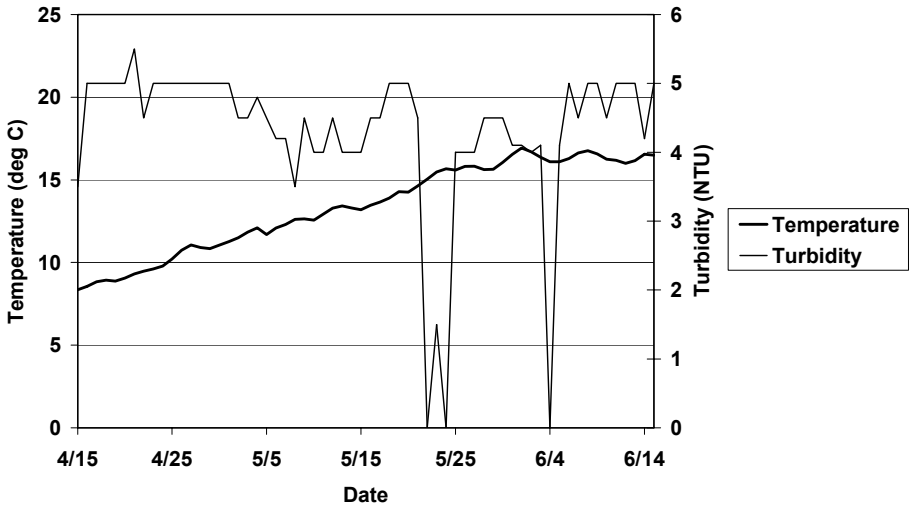

Figure 7. Temperature and turbidity from 15 April – 15 June 2001 at TDA. Data were obtained from DART, an Internet website (http://www.cqs.Washington.edu/DART/). (The zero NTU values for turbidity are suspect.)

Smolt Migration Characteristics

Data on smolt migration characteristics at TDA were based on the Smolt Monitoring Program's (SMP) sampling at John Day Dam. This is the closest SMP facility upstream of TDA; SMP sampling is not conducted at TDA. The data were not lagged because travel times between John Day and TDA are relatively fast (generally < 1 d, based on radio telemetry data, John Beeman, U.S.G.S. Biological Resources Division, pers. comm.).

Our study encompassed most of the migrations of yearling steelhead and coho, and roughly half of the yearling (stream-type) chinook salmon (Figure 8). The migration of subyearling (ocean-type) chinook salmon and of sockeye occurred after the study's end, June 1. Passage of steelhead, yearling chinook and coho peaked on May 1, May 17 and May 23, respectively (Figure 8). Passage of the most abundant salmonid fish migrating downstream through John Day Dam, subyearling chinook, peaked in mid-summer (smolt index of 100,000). During our study (April 24 to June 1), yearling chinook (72.1%) were the most abundant juvenile salmonid, followed by steelhead (19.8%), coho (5.3%), sockeye (2.0%), and subyearling chinook (0.8%) salmon.

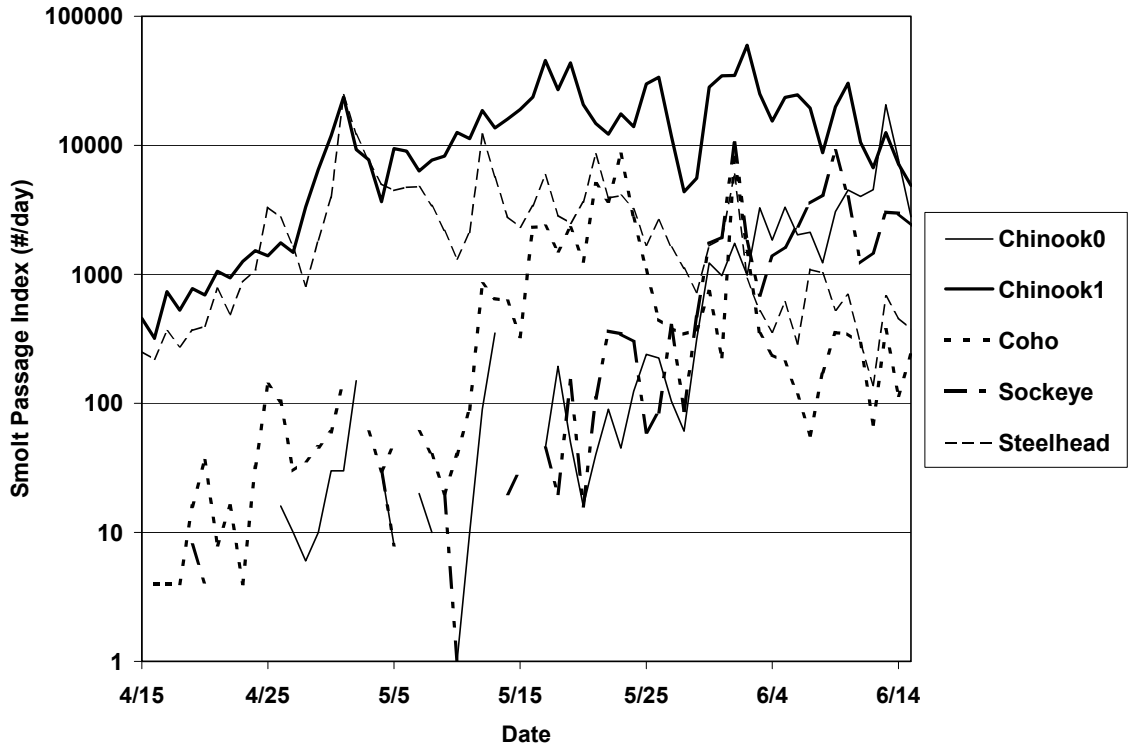

Figure 8. SMP index (logarithmic scale) from John Day Dam for 15 April – 15 June 2001. Designations in the legend are for subyearling chinook salmon (Chinook0), yearling chinook salmon (Chinook1), coho salmon, sockeye salmon, and steelhead. Data were obtained from DART, an Internet website (http://www.cqs.Washington.edu/DART/).

Section 3: METHODS

Our general approach was to intensively sample fish movements in the region immediately upstream of a sluiceway entrance at TDA. We used an active fish tracking sonar (AFTS), commonly called a sonar tracker, to obtain fish movement data. AFTS as applied at a dam (described below) was first discussed by Hedgepeth and Condiotty (1995), and later published in BioSonics (1996), Hedgepeth et al. (1999) and Hedgepeth et al. (2000). AFTS was also a key element in the Behavioral Acoustic Tracking System that is used to track acoustic-tagged fish (Johnson et al. 1998). MacLennan and Simmonds (1992) explain split-beam hydroacoustics, a main component of AFTS.

Data Collection

AFTS System

The components of an AFTS system (BioSonics 1998) (Figures 9 and 10) include a 208 kHz BioSonics DT4000 digital split-beam echo sounder, a 7° split-beam transducer, two high-speed stepper motors for dual axis rotation, a controller unit, a laptop computer, a desktop computer, and cables. AFTS calibration and other technical data are in Appendix A. See Johnson et al. (2001) for an error analysis of AFTS.

AFTS is based on the principle of tracking radar. Appendix B provides an algorithmic description of AFTS, and a simple description follows. Once a fish was detected after the transducer was randomly aimed into the sample volume, two high-speed stepper motors aligned the axis of the digital split-beam transducer on the target. As the fish moved from ping to ping, deviation of the target from the beam axis was calculated and a predictive tracking algorithm was applied to re-aim the transducer, thereby tracking the target. The predictive tracking algorithm was a discounted least-squares fit (Brookner 1998), where the most recent velocity estimate (magnitude and direction) was weighted by unity, the next most recent by one-half, the next by one-fourth, the next by one-eighth, and so on. If no target was detected after 30 sec of pinging at a given position, the aiming angles were changed to another random position. The ping rate was approximately 10 pps. The echo sounder threshold was set at –60 dB on-axis. For each ping the target was tracked, data on fish X, Y, Z position relative to the transducer and target strength were recorded to disk. Fish position resolution can be

inferred from the angular resolution (± 0.35°). At 10 m from the transducer, this would amount to ± 6 cm, and at 1 m the error would be ± 0.6 cm.

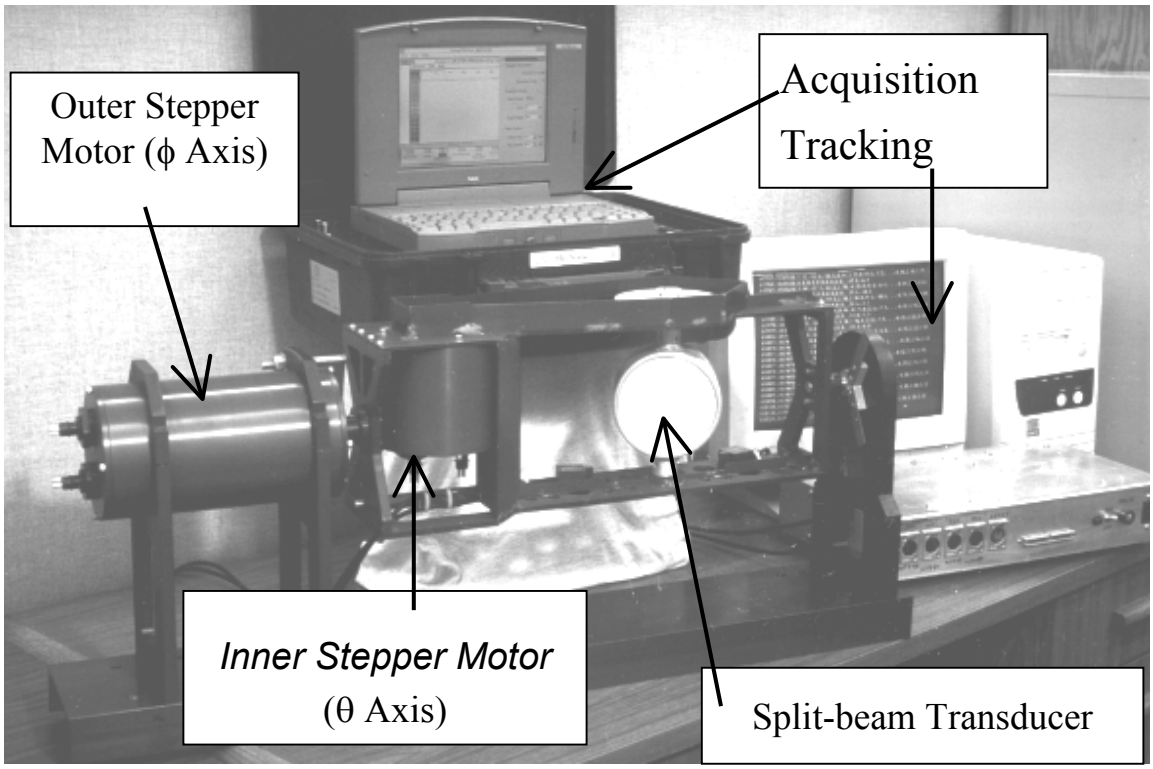

Figure 9. Photograph of the active fish tracking sonar.

Two AFTS systems were deployed at Main Unit 1-2. One was mounted on the tip of the J-extension to sample fish movements when the J-occlusions were in place. The other was mounted about 20 m deep on a trashrack to sample fish movements when the J-occlusions were out of the water. The primary area of interest for both trackers was a region 10 m wide, 15 m from the dam, and 10 m deep immediately in front of Sluice 1-2. We measured the position of the transducers relative to Corps of Engineers survey point TDP-1 on the pier nose at FU 2-2/MU 1-1. The location of TDP-1 was Northing 711330.743 ft, Easting 1839844.001 ft, and elevation 185 ft (Oregon State Plane N, NAD 27 horizontal datum and NGVD 29/47 vertical datum). The AFTS transducer on the J-occlusion was located 12.36 m along the powerhouse 13.72 m into the forebay and -21.09 m down from TDP-1 (Northing 216832.062 m, Easting 560783.875 m and elevation 35.618 m). The location of the AFTS transducer on the trashrack was located 13.20 m along the powerhouse 6.86 m into the forebay and -28.96 m down from TDP-1 (Northing 216827.703 m, Easting 560789.188 m and elevation 27.428 m).

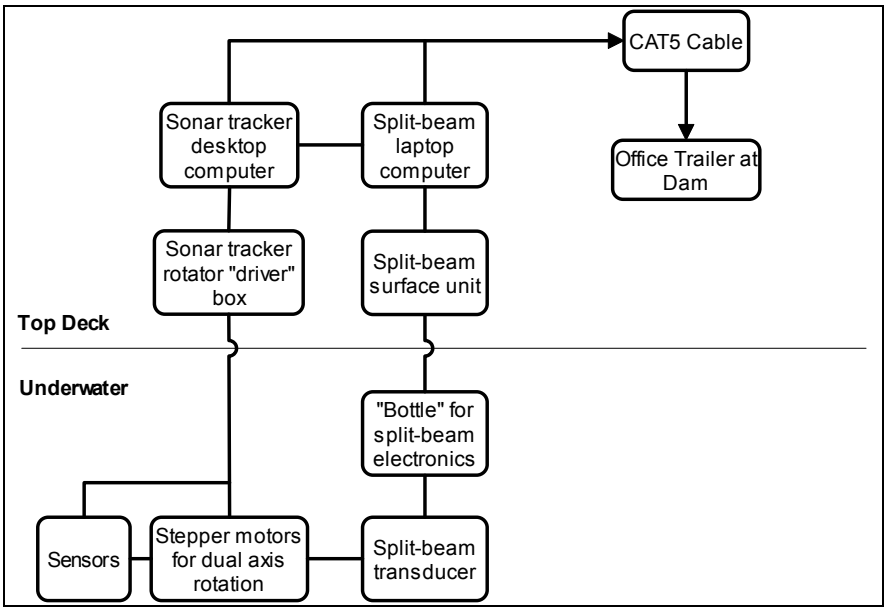

Figure 10. Schematic showing AFTS, with tracker and split-beam components, and data flow via network (CAT-5) cable from the equipment shed at MU 1-2 to an office trailer at the dam. Two of these systems were deployed.

Sample Volume

With the J-occlusions IN, the sample volume for the sonar tracker deployed on the tip of the J-section incorporated the region in front of Sluice 1-2 from the surface to the J-section and out about 18 m into the forebay (Figure 11). The sample volume dimensions with the J-occlusions IN are summarized in Table 1.

With the J-occlusions OUT, the sample volume for the sonar tracker deployed on the trashrack at elevation 90 ft incorporated the region in front of Sluice 1-2 from the surface to the transducer and out about 16 m into the forebay (Figure 11). The sample volume dimensions with the J-occlusions OUT are summarized in Table 1. The sample volumes are not identical between J-occlusion treatments because of differences in tracker location (IN tracker on J-tip and OUT tracker on trashrack).

Table 1. Boundaries of the actual sample volumes by dimension for J-occlusions IN/OUT and spill/no spill. (Too few data were available to include the condition of J-occlusions OUT and spill.) The data (in meters) are referenced to "dam coordinates" with the origin at the Intake 1-2 centerline at the plane of the pier noses at the water surface (elevation 158 ft). Positive X is to the east, positive Y is away from the dam, and positive Z is upward in the water column.

J-OCCLUSIONS	SPILL	X	Y	Z
IN	No	-4 to +4 m	+3 to +18 m	-0.5 to –8 m
IN	Yes	-4 to +3 m	+4 to +14 m	-0.5 to –5 m
OUT	No	-2 to +6 m	+4 to +16 m	-0.5 to –8 m

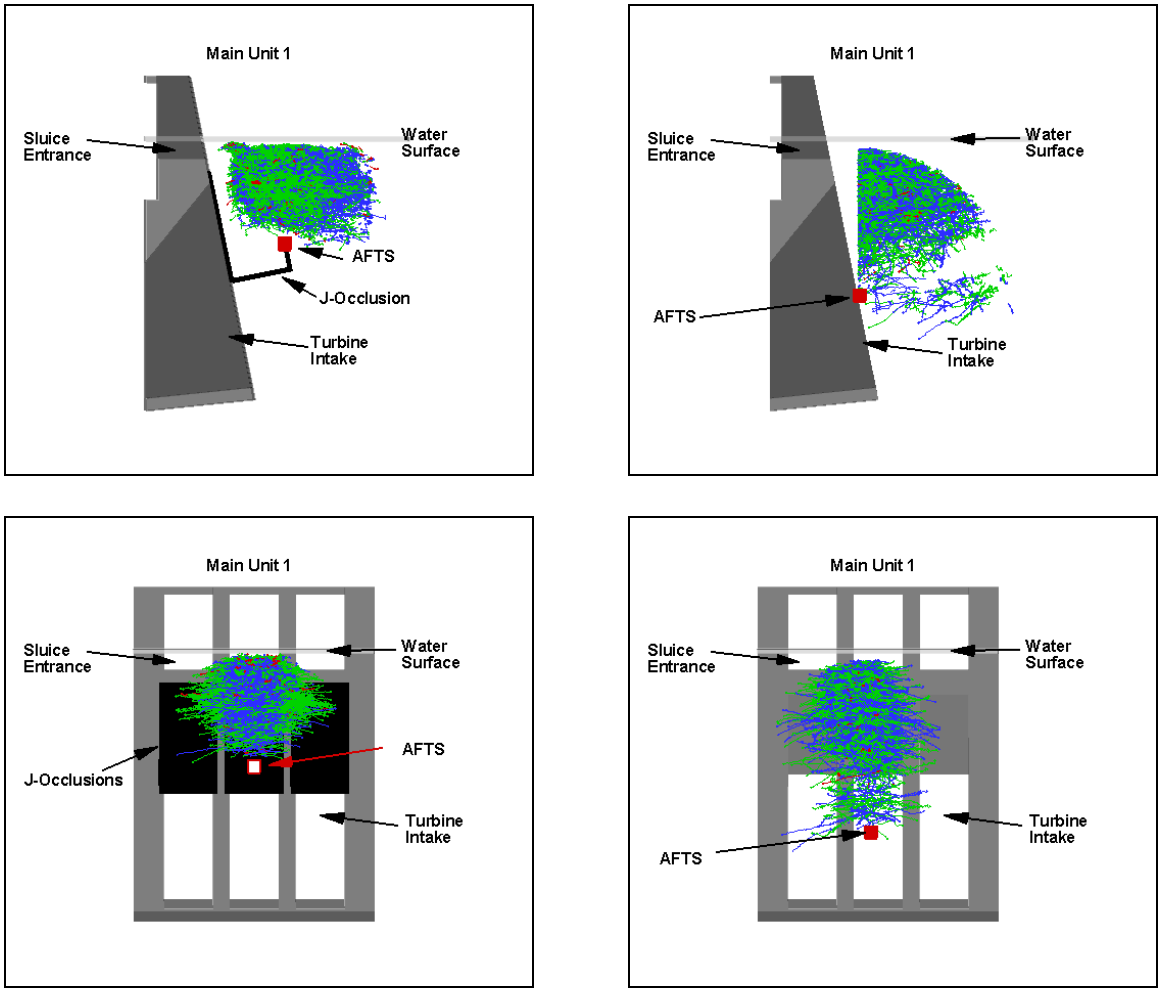

Figure 11. Side and front views of sample volumes for conditions with (left figures) and without (right figures) J-occlusions.

Experimental Factors

Overall, data were collected on 32 of 39 possible days (Table 2). We tracked about five times as many fish in the IN condition than the OUT (Table 2). The total of ~46,000 tracked fish was about half the total number tracked in the 2000 study.

The experimental design for the J-occlusion evaluation (fixed hydroacoustic and radio telemetry studies were also undertaken) called for 3-day treatments (occlusions IN or OUT) randomized in 6-day blocks. Difficulties with raising the J-occlusion early in the study precluded completion of the experimental trials as planned (Table 2). Instead, overall observations were made with the J-occlusions IN and OUT. And, on May 16 about half way through the study, dam operations abruptly changed as 30% spill 24 h/d was enacted.

Table 2. Summary of sonar tracker data collection by study-day when data were collected at TDA in 2001.

SPILL	PERIOD	J-OCCLUSIONS	DATE	NO. TRACKS
NO	1	IN	24-Apr	414
			25-Apr	879
			26-Apr	1317
			27-Apr	2150
			28-Apr	2070
			29-Apr	2770
			30-Apr	839
	2	OUT	1-May	557
			2-May	2251
			3-May	1966
			4-May	1368
			5-May	772
	3	IN	5-May	739
			6-May	3030
			7-May	3388
			8-May	1731
			9-May	1970
			10-May	2192
			11-May	1289
	4	IN	14-May	2096
		(cont' next page)	15-May	2793

			16-May	2651
YES			17-May	732
	5	OUT	21-May	150
			22-May	322
	6	IN	23-May	229
			24-May	949
			25-May	773
			26-May	308
	7	IN	29-May	570
			30-May	1203
			31-May	1214
			1-Jun	377

Statistical analysis in the context of a formal experimental design will not be appropriate for these data because the replication necessary for statistical testing was not realized. Thus, quantitative statistical tests will not be conducted. Furthermore, we do not have seasonal "blocks" in the statistical sense, however, we do have observational "periods" under different test conditions (Table 2). In conclusion, there are three analysis factors that can be examined qualitatively.

- J-occlusions IN/OUT
- Day/Night
- Spill/No spill

Data Reduction and Analysis

Data reduction and analysis steps are shown in Figure 12. Hydraulic data were not available; thus, the analysis included only observed fish movement data. Typically, day and night periods (see definitions below) were analyzed separately because of known day/night differences in sluice passage (Ploskey et al. 2001b).

The tracking data from AFTS (TXT files) were filtered for minimum number of echoes per track (10) using a C-compiled program called TRKPROCA.EXE. The TRA output files from this program were reduced in a SAS-program called EDITQC.SAS, which removed unnecessary auxiliary information. The TRA files were also manually edited to delete fish track data for the 30 min period before any system crashes because

AFTS performed a positioning self-check every 30 min to check for slippage in rotator position during data collection. If there was slippage, AFTS stopped collecting data and waited to be re-started. This occurred seven times during the 73 days data were collected. Thus, data 30 min before these seven events could be erroneous and had to be deleted. The daily output files from the editing process were called TR1 files.

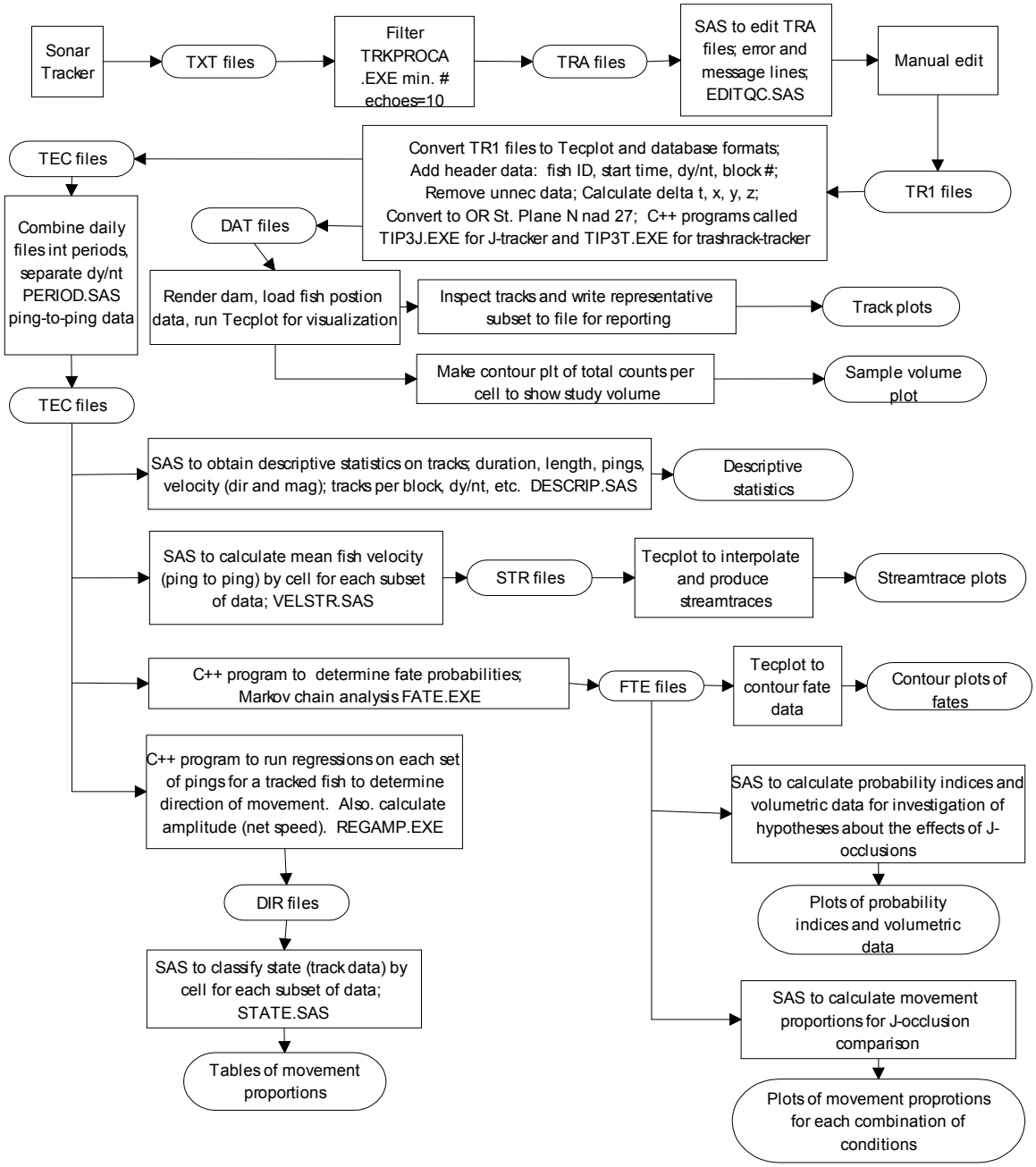

Figure 12. Data flow chart.

The daily TR1 files were processed using a C-compiled program called TIP3D.EXE. Two daily output files were produced: DAT files formatted to be loaded into Tecplot software (Amtec Engineering, Inc. Bellevue, Washington) and TEC files for further data and statistical analysis. Data processing by TIP3J for the J-tracker and TIP3T for the trashrack tracker included:

- Reassemble tracks – Separate tracks adjacent in time and space were reassembled. This usually occurred when AFTS automatically broke-off tracking when the maximum number of echoes per track was reached (800), or when maximum number of missing pings was reached (20).

- Fish track identification number – The purpose here was to give each track a unique identification number for subsequent data analysis. A fish track identification number was made from the date and an integer starting at 1 and proceeding consecutively.

- Day/night determination – Sunrise and sunset times for each date during the study period were obtained from the U.S. Naval Observatory website (http://aa.uno.navy.mil/AA/data/). The time of the start of a given fish track was then compared to the sunrise/sunset times to determine if the track was in day or night. A day/night designator was then written to the output file: day = 0 and night = 1.

- Delta X, Y, Z, T calculations – The difference in three-dimensional fish position (X, Y, Z) and time between consecutive echoes in a track was calculated as follows, using delta X as an example between the i and i+1 echoes of the track:

$$\Delta X = X_{i+1} - X_i$$

- Conversion to dam coordinates – The raw position data are in “tracker” coordinates, i.e., relative to the location of AFTS’s split-beam transducer and rotators (centered at intersection of axes). This Cartesian coordinate system was converted to “dam” coordinates for the purposes of display and analysis. The origin of the “dam” coordinate system (see Figure 11) was the center of the MU1-1/FU2-2 pier nose at Elevation 48.2 m (158 ft).

- Conversion to Oregon State plane coordinates – Similarly, the raw position data were also converted to Oregon State Plane NAD 27 coordinates. This is the same coordinate system that other researchers and CFD modelers will use.

We used Tecplot software to visualize the fish tracks obtained from AFTS. To do this, we first rendered the dam in Tecplot. Then the specific tracks contained in the DAT files from the TIP3 programs were turned into "zones" in Tecplot. The tracks were superimposed on the dam rendering, both of which were in "dam" coordinates. Tecplot visualization allowed us to manipulate and explore the three-dimensional nature of the tracks relative to the dam.

Descriptive data on the data set were obtained using the SAS-program DESCRIP.SAS. Using the TEC files as input, DESCRIP.SAS produced the following data for each day/night period in each treatment:

- number of observations (distinct fish positions);
- mean, minimum, and maximum number of echoes per track;
- mean, minimum, and maximum positions in the X, Y, and Z dimensions;
- mean, minimum, and maximum velocities in the X, Y, and Z dimensions.

Streamtrace analysis based on ping-to-ping estimated velocities

Ping-to-ping velocity data averaged within each 0.5 m cell were the basis for the mean velocity analysis and the streamtrace analysis. Mean velocities over the entire sample volume were obtained for each study period for each dimension (X, Y, and Z) for day and night separately. Using the base data set of mean X, Y, Z velocities by 0.5 m cell, streamtraces were generated using steamtrace algorithm in Tecplot for X/Y and Y/Z velocity vectors separately. All subsequent data analyses were based on fish track data, not ping-to-ping data.

Direction of movement based on identified fish tracks

Fish track directionality relative to the presence of J-occlusions, night versus day and spill condition can be characterized using proportions based on individual track regressions in each of the three dimensions: along the dam, upstream/downstream and up/down. The movement proportions were based on the results of linear regressions applied on each fish track for each dimension separately to estimate three components of movement, as in the following example for the X-dimension:

$$Position_x = a_x + b_x\left(Time\right)$$

where, a_x and b_x are the y-intercept and slope coefficients of the linear regression for the X-dimension. Linear regression though all positions comprising a track was more representative of track movement in its entirety than data from just the end points (Figure 13).

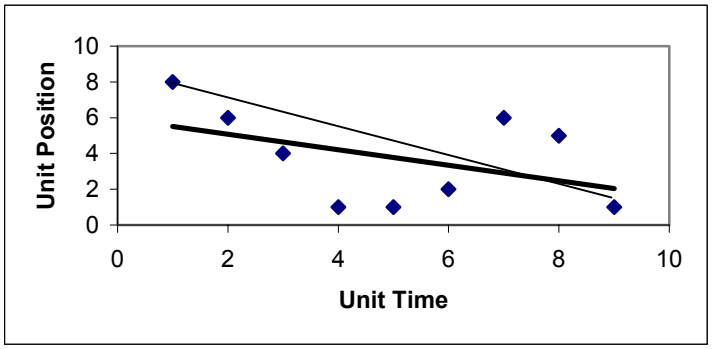

Figure 13. Example fish track data showing linear regression line (solid black) and line through end points (thin black).

Tracked fish in the resulting data set were allocated to 1.0 m cells in the sample volume. Proportions of fish moving in each of three dimensions were calculated for each cell. These movement proportions were then the basis for a comparison of movements with and without J-occlusions in place. A common sample volume was selected across all combinations of J-occlusion plates IN/OUT, day/night, and spill/no spill.

Summary proportions and variances were calculated for direction of movement separately for each dimension (X east/west; Y toward/away; Z up/down) for each condition (J-occlusions IN/OUT, day/night, and spill/no spill) as follows:

$$p_i = \frac{a_i}{m_i}, \text{ the estimated proportion on day } i \ (i = 1,\ldots,n),$$

where a_i is the number of tracked fish with a particular sign of regression slope (positive or negative) and m_i is the total number of tracked fish. The overall estimate across n-days of a particular treatment condition is

$$p = \frac{\sum_{i=1}^{n} a_i}{\sum_{i=1}^{n} m_i}$$

with associated estimated variance

$$Var(p) = \frac{1-f}{n\bar{m}^2}\left[\frac{\sum_{i=1}^{n} a_i^2 - 2p\sum_{i=1}^{n} a_i m_i + p^2\sum_{i=1}^{n} m_i^2}{n-1}\right]$$

where f=0 (i.e., the fpc is ignored) and where

$$\bar{m} = \frac{\sum_{i=1}^{n} m_i}{n}.$$

Markov analysis of fates based on identified fish tracks

For the purpose of this study, a fate is specified by where fish tracks exited the sample volume. Fates are expressed as probabilities of passage toward a particular area, e.g., the sluiceway. To determine fate probabilities, we applied a Markov analysis (Taylor and Karlin 1988, pp. 95-266), which described smolt movement as a stochastic process. A couple key ideas from Taylor and Karlin (1998, pp. 95-96) are: (a) a Markov process $\{X_t\}$ is a stochastic process with the property that, given a value X_t, the values of X_s, for s>t are not influenced by the values of X_u for u<t, and (b) transition probabilities are functions not only of the initial and final states, but also of the time of transition as well. When the one-step transition probabilities are independent of the time variable, then the Markov chain has stationary probabilities. The Markov-chain analysis for the 2001 TDA sonar tracker study included the following assumptions.

- The movements can be described by a one-step Markov process. In other words, movement decisions are based on the smolt's current position and not upon the prior history getting to that position.
- The transition probabilities are estimated from independent fish observations.

- The transition matrix is stationary.

As with the state analysis, the three-dimensional sample volume in front of Sluice 1-1 was divided into cells (modified for fate analysis as follows: 0.5 x 0.5 x 0.5 m for X, Y, Z, respectively). The sample volume was decreased to reduce the size of the Markov matrices: X = -3.0 to 3.0 m, Y = 3.0 to 15.0 m, and Z = –6.0 m to –0.5. At the boundaries (sides) of the volume, we defined these passage fates:

- Sluice – cells on side facing the sluiceway, 0.0 to 4.0 m deep;
- Turbine – cells on side facing the sluiceway, 4.0 to 6.0 m deep;
- West – west side cells;
- East – east side cells;
- Bottom – bottom cells of the volume;
- Reservoir – cells of side facing the reservoir upstream;
- Unknown – no movement.

The Markov transition matrix was a square matrix the size of k x k, where k is the number of distinct cells being modeled (k = 4,080). The *ij*th element in the *i*th row of the *j*th column of the transition matrix was the estimated probability (p_{ij}) of moving from cell i to cell j in the next time step. These probabilities were estimated by:

$$\hat{p}_{ij} = \frac{x_{ij}}{n_i}$$

where,

n_i = number of observations of smolts in the *i*th cell;

x_{ij} = number of observations where a smolt in cell *i* moved to cell *j* in the next time step.

The cells (0.5 x 0.5 x 0.5 m) that bordered the sides of the volume of interest (sluice, turbine, west, east, bottom, and reservoir) were set to unity to absorb any movement that reached a particular “fate.” Otherwise, C-compiled programs (FATEJ.EXE for the tracker on the J-occlusion and FATET.EXE for the tracker on the

trashrack) tallied the transition matrix T using a time step of 1 sec, and the average position (i.e., $\sum x_t / n$) during each 1 s interval a fish was tracked. This program required that a fish be tracked for at least two seconds before the transition matrix was amended to obtain indices *i* and *j* (*i* from the first interval, *j* from the second). Non-boundary (including surface) cells were checked to ensure non-zero and non-unity values. If zero or unity was present in an *i*,*i* cell after building the matrix T from a set of data, then the closest *i*,*i* cell in Cartesian space was found that contained data and was used to augment that particular set of *i*,*j*'s. This process created a situation that guaranteed fish movement to one of the absorbing boundaries if there was movement to begin with.

The transition matrix T for one time step was then used to estimate the transition for two or more time steps as:

$$T^t$$

where, t = the number of time steps. For this study, t = 4,096 so that the Markov process reached stability, i.e., the transition matrix did not change with additional time steps. The ultimate fate of smolts would be calculated as:

$$T^{4096}.$$

After 4,096 time steps (corresponding to 68 min), probabilities for each of the seven fates for each of the 2,970 cells, not including border cells, were extracted from the transition matrix and written to file. The fate data were displayed in Tecplot.

The key assumption in this analysis is that the data exhibit the Markov property (see first assumption above). The one-step model we used in the analysis of day and night fish movement assumed movement to a future cell depended entirely on the fish's current position, not its prior history. However, movement could depend on both the current and past histories. A R x C table was used to test whether movement from B to C_i is independent of previous position A_i. As many cells as were practical were tested in this manner. Movement and cells were measured using a time step of 1 s and 0.5 m per side cells with x values from 1 to 6.5 m (*i*=0…10), y values from 1 to 6.5 m (*i*=0…10), and z value from –3.5 to –0.5 m (*k*=0…5). Cell codes were formed as *i*+*j**11+*k**121. A Chi-Square test was not valid due to the sparseness of the contingency tables.

Therefore, conclusions about appropriateness of the first order assumption of a one-step Markov process were based on Fisher's exact test (Sokal and Rohlf 1981, p. 740). Cells where the number of fish positions was greater than 10 were tested in this manner. A total of 270 cells during daytime and 226 during nighttime out of the possible 726 were tested from the 2000 data set.

In general, movement was tested to be independent of prior position. P values less than 0.05 showed significance in 24 (8.9 %) of the cases during daytime and 18 (8.0%) of cases at night. That is, the null hypothesis of lack of association was rejected in fewer than 9% of the cases examined. This is a good indication that our use of the Markov-Chain was appropriate for characterizing movement through the volume near Sluice 1-2.

Probability Indices and Volumetric Analysis

In addition to comparing fish movements in general for various conditions, we were interested in assessing specific hypotheses about the effects of the J-occlusions on fish movements in the nearfield of Sluice 1-2. After congruent sample volumes for each combination of conditions were established, we used the fate probabilities from the Markov-chain analysis to calculate "probability indices." A probability indices (*PI*) for a given condition will simply be the average fate probability over all cells in the sample volume, as follows:

$$PI = \frac{\sum_{i=1}^{m}\sum_{j=1}^{n}\sum_{k=1}^{o} F_{i\,jk}}{m \cdot n \cdot o}$$

where, F_{ijk} is the fate probability for the ith cell along the dam the jth cell away from the dam, and the *k*th cell deep.

In addition, we calculated the volume ($VTOT_F$) under each condition where the fate probabilities (F) were equal to or greater than 0.7, 0.8, and 0.9:

$$VTOT_F = V_{cell}\sum_{i=1}^{p}\sum_{j=1}^{q}\sum_{k=1}^{r} F_{ijk}$$

where, $F_{ijk} \geq F$ and V_{cell} is the volume per cell.

Section 4: RESULTS

The 2001 study results include track description, fish velocity and steamtraces, direction of movement proportions, movement fates, comparison of J-occlusions in and out, and evaluation of hypotheses about J-occlusion effects. The results are typically presented separately for the various combinations of treatment conditions, e.g., J-occlusions IN/day/spill.

Track Description

Fish tracks from AFTS can be described using example tracks, track length, and average number of pings per track. Example tracks with the J-occlusions IN and OUT show similar patterns (Figure 14). Tracked fish generally were moving toward the dam and upward in the water column (diamonds in Figure 13 depict the end of each track). Track length varied with short (~1 m) tracks interspersed with long (~5 m) tracks, as shown in the scaled Figure 14. The number of pings per track was somewhat lower for the deployment with J-occlusions IN (43 pings/track) than with them OUT (50 pings/track) (Table 3). As in 2000, the number of pings per track was higher during night than day (Table 3).

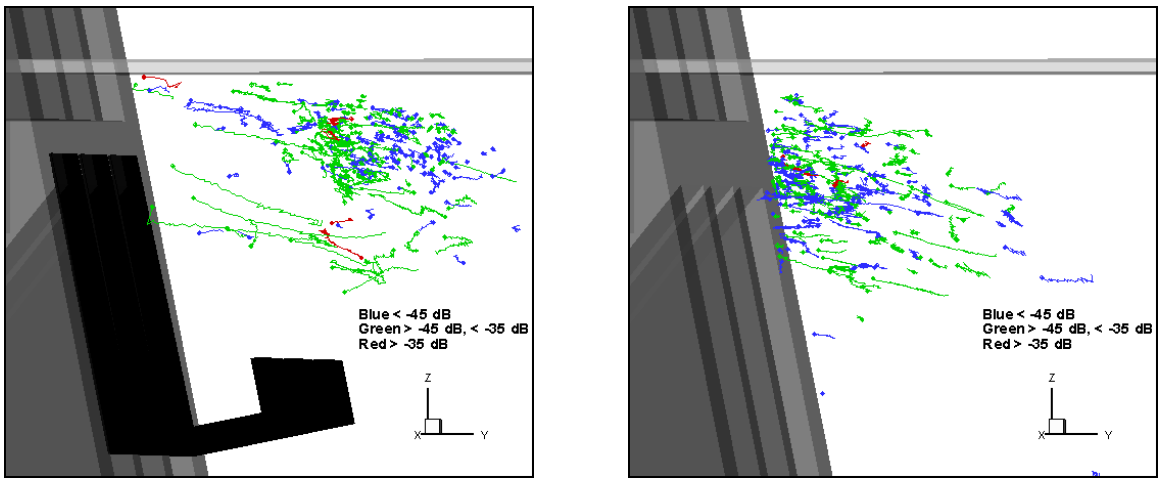

Figure 14. Isometric view of example tracks with (left figure) and without (right figure) J-occlusions. Data are from the first 250 tracks collected on April 28 and May 2 for J-occlusions IN and OUT, respectively.

Table 3. Descriptive track statistics separately for J-occlusions IN and OUT.

		IN	OUT
Day	Pings	579,801	191,904
	Tracks	16,402	4,146
	Pings/track	35	46
Night	Pings	963,296	291,053
	Tracks	19,831	5,450
	Pings/track	49	53
Combined	Pings	1,543,097	482,957
	Tracks	36,233	9,596
	Pings/track	43	50

Mean Fish Velocity

Mean fish velocities in the three dimensions were comparable for J-occlusions IN and OUT for periods with the same spill condition (Figure 15). Patterns between day and night similar except velocity magnitude was greater for day than night. The most important observation from the fish velocity data was the noticeable shift in velocity that occurred between periods 4 and 5 when spill changed from off to on; mean velocity in the X-dimension went from ~0.0 to ~-0.2 m/s during day and from ~0.0 to –0.07 m/s at night. Thus, movement to the west was stronger with spill than without. Also, there was stronger movement toward the dam (Y-dimension, e.g., from –0.05 to –0.07 m/s during day) and upward in the water column (Z-dimension, e.g., from 0.0 to ~0.02 m/s during day) after spill was initiated, although the magnitudes of these shifts were less than it was for the X-dimension. Spill seemed to have more of an effect on fish velocity in front of Sluice 1-2 than the J-occlusions (Figure 15).

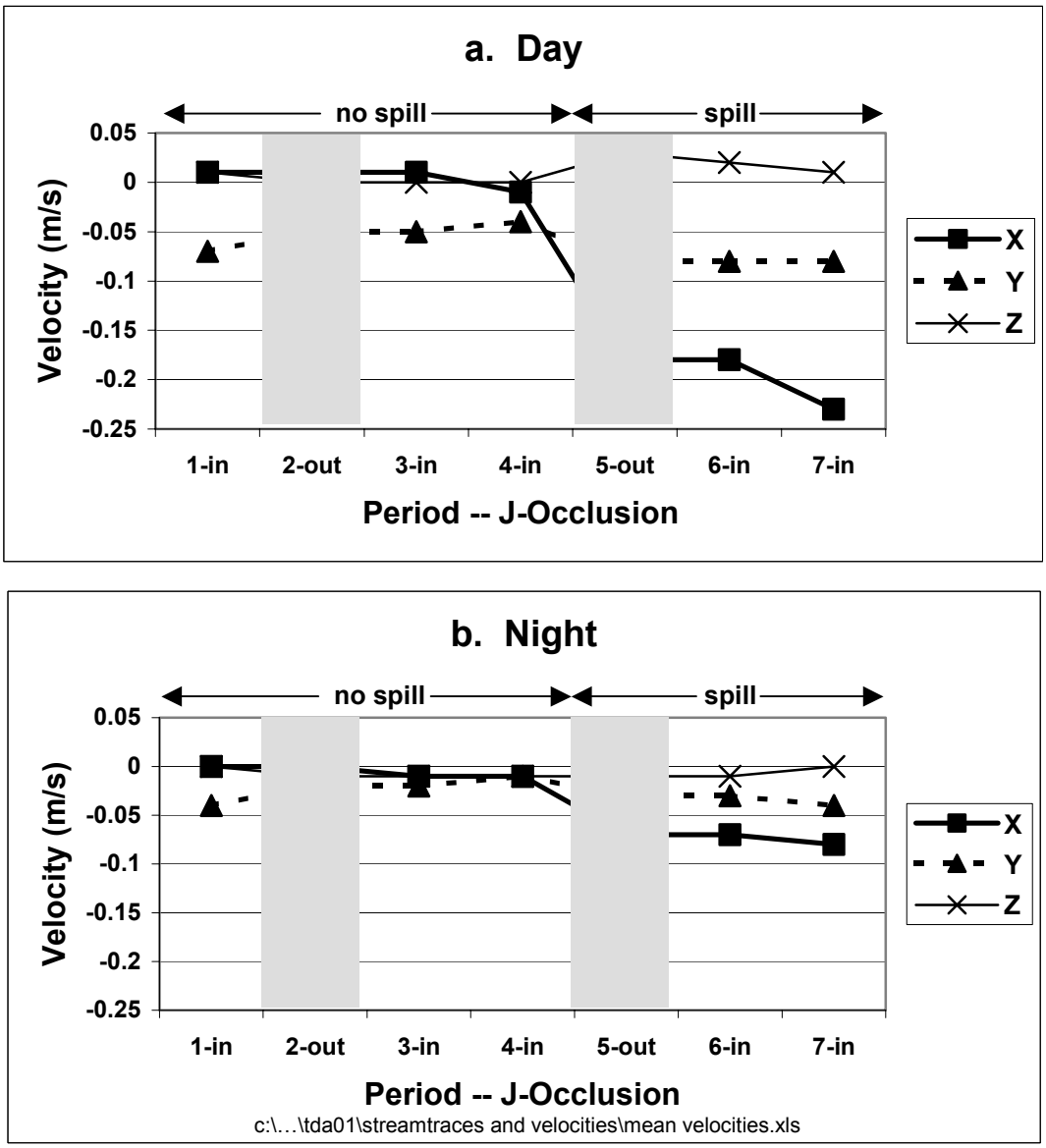

Figure 15. Mean observed fish velocity data by period (defined in Table 1) for day and night separately. Shaded areas are data for J-occlusions OUT. Positive X is to the east, positive Y is away from the dam, and positive Z is upward in the water column. Periods 1-4 had no spill; periods 5-7 had spill.

Streamtraces

Observed fish velocities, which we averaged over the $(0.5\ m)^3$ cells of the sample volume, are presented in contour plots (Figures 16, 17, and 18) for each dimension separately to show movement relative to the entrance for Sluice 1-2 (X is horizontally, Y is longitudinally, and Z is vertically). Streamtraces based on the cell by cell average fish velocity data were superimposed on the contour plots of velocity magnitude. Streamtraces depict the direction of two-dimensional fish velocity vectors. The data are from 3 m "slices"; the side views are for a slice centered on Sluice 1-2 and the plans views are for the 0.5-3.5 m depth layer. Any differences in the magnitude and direction of fish velocities in this particular region between J-occlusions IN and OUT will be indicated in this analysis.

No noticeable differences in fish velocity patterns were observed between the J-occlusions IN and OUT conditions whether during day (Figure 16) or night (Figure 17) in the no spill period. In addition, similar velocity patterns between day and night were observed during the spill period (Figure 18). (Recall, the IN/OUT comparison could not be made for the spill period because the amount of data for J-occlusions OUT was insufficient for analysis.) The fish velocity and streamtrace analysis produced the following findings.

- X-velocity showed the most striking pattern of the three velocity components. During the no spill period, X-velocity was eastward east of the Sluice 1-2 centerline and westward on the west side of the centerline (Figures 16 and 17). X-velocity was highest at the edges of the analyzed volume. During the spill period, a completely different pattern was observed (Figure 18) with strong westward velocities throughout much of the volume, as we saw with the mean velocities in Figure 15.
- Y-velocity was almost always toward the dam (Figures 16, 17, and 18). It was strongest within 7-8 m of the dam in the surface layer 5-6 m deep.
- Z-velocity was generally upward within 10 m of the dam, but downward at distance greater than 10 m (Figures 16, 17, and 18). The magnitude of upward velocity was highest in the sample areas closest to the sluice entrance.
- Streamtraces revealed movement toward Sluice 1-2 within 6-7 m of the entrance during no spill (Figures 16 and 17), but not during spill (Figure 18).

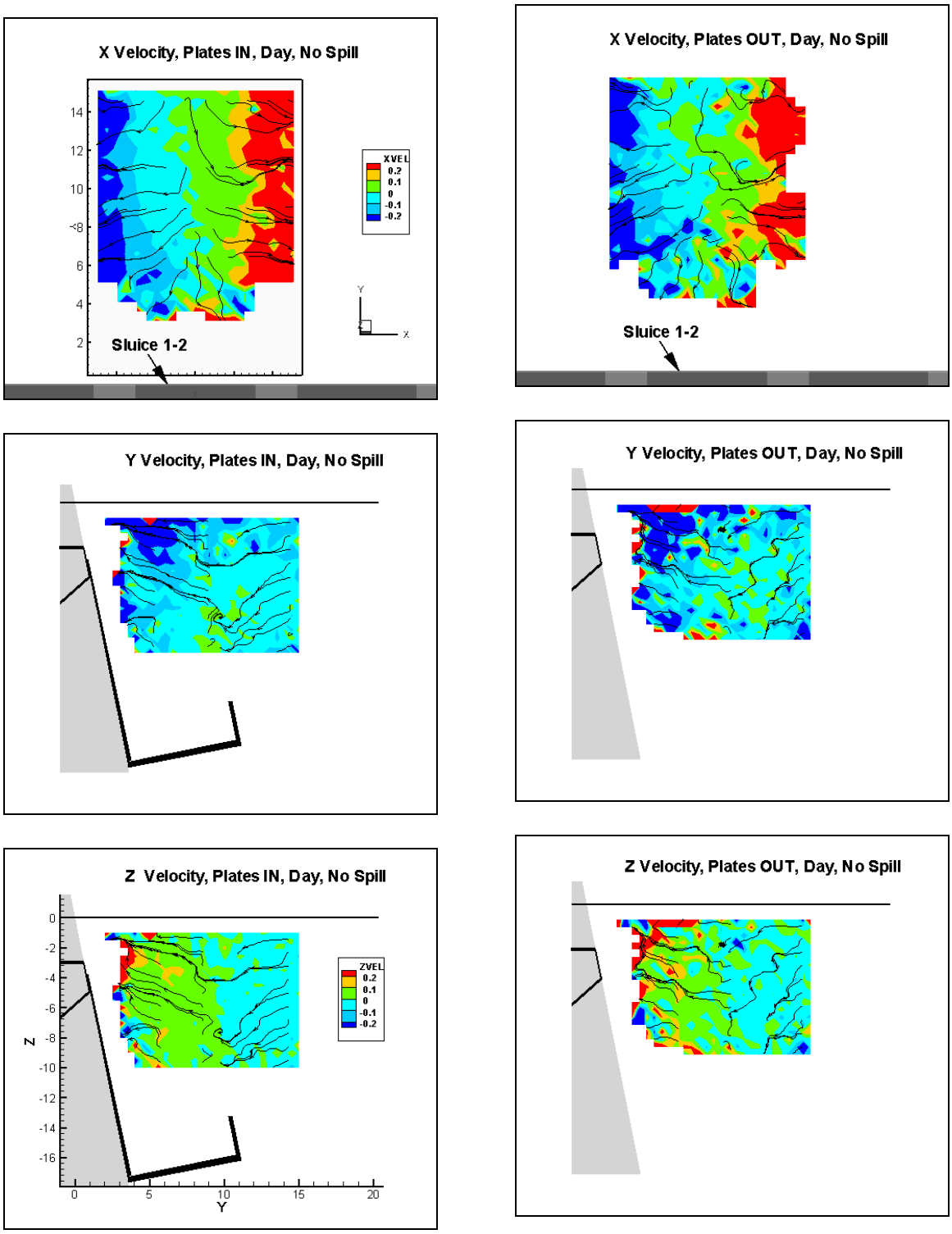

Figure 16. Fish velocity contour plots with derived fish streamtraces comparing J-occlusions IN (left column) vs. OUT (right column) for day, no spill.

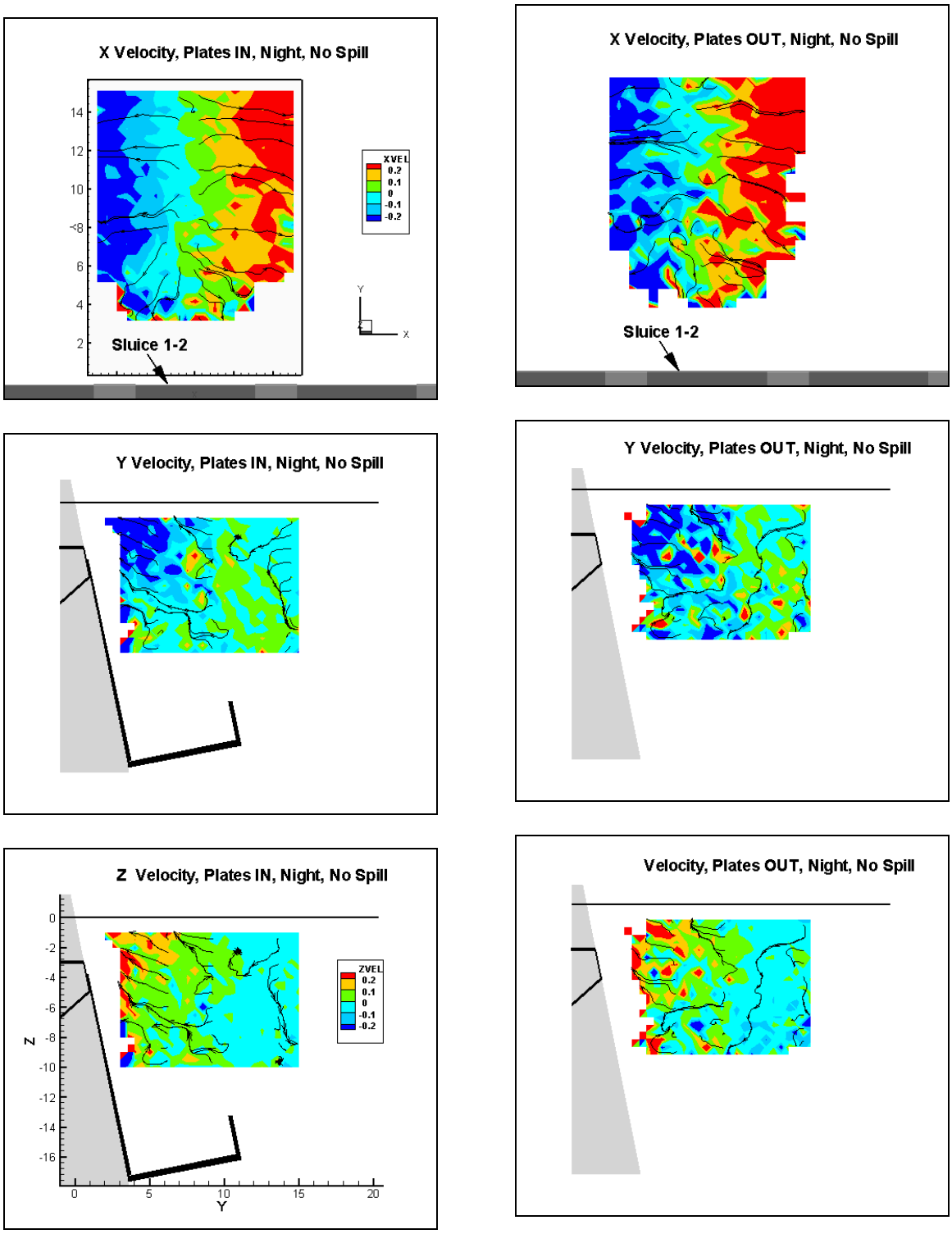

Figure 17. Fish velocity contour plots with derived fish streamtraces comparing J-occlusions IN (left column) vs. OUT (right column) for night, no spill.

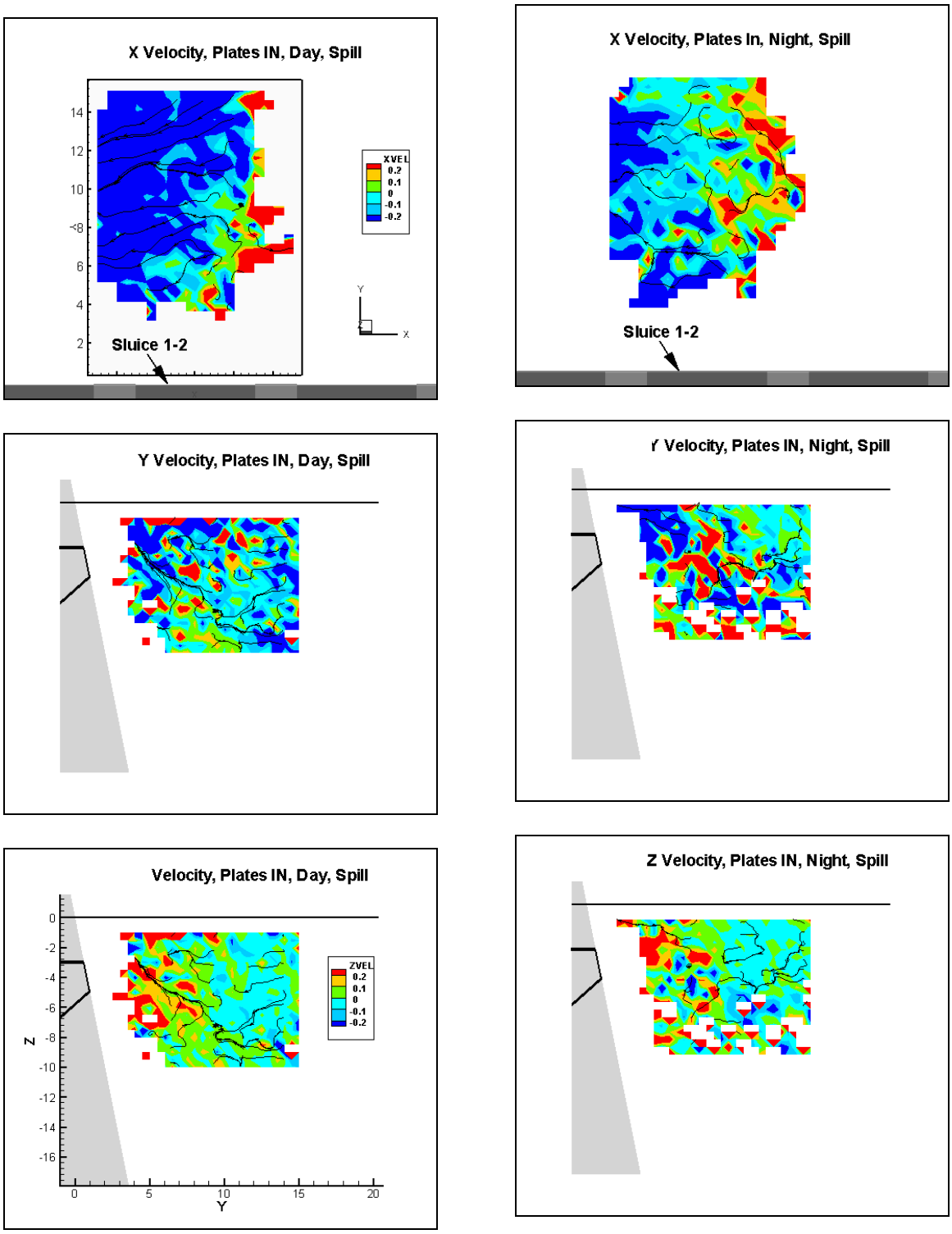

Figure 18. Fish velocity contour plots with derived fish streamtraces comparing day (left column) vs. night (right column) for J-occlusions IN, spill.

Direction of Movement Proportions

Fish track directionality relative to the presence of J-occlusions can be summarized using proportions of movement based on individual track regressions in each of the three dimensions. The proportion of fish moving westward toward the spillway (out of the total west plus east; the X-dimension) was about the same with (0.52±0.02) and without (0.51±0.03) J-occlusions (Table 4). The proportion of fish moving toward the dam (out of the total toward plus away; the Y-dimension) was the same (0.58±0.02) whether the J-occlusions were IN or OUT (Table 4). And, the proportion of fish moving upward (out of the total up plus down; the Z-dimension) was slightly higher with J-occlusions IN (0.50±0.02) than OUT (0.48±0.02) (Table 4). In general, movement proportions toward the dam and upward were 0.03 to 0.04 higher during day than night.

As seen previously, however, the most dramatic effect on fish movements in front of Sluice 1-2 was caused by spill. When water was spilled, movement proportions toward the dam and upward were 0.03 to 0.04 higher during spill than no spill. Also during spill, the proportion of fish moving westward toward the spillway was 0.64 compared to 0.50 during no spill. This implies that spill may have diminished sluiceway efficiency by drawing fish to spill that might otherwise have passed into the sluiceway.

Table 4. Summary mean proportions with 95% confidence levels for direction of movement separately for each dimension (X, Y, Z) for J-occlusions IN, OUT, day, night, no spill, and spill.

	X		Y		Z	
	EAST (+)	WEST (-)	AWAY (+)	TOWARD (-)	UP (+)	DOWN (-)
IN	0.48 ±0.02	0.52 ±0.02	0.42 ±0.01	0.58 ±0.01	0.50 ±0.02	0.50 ±0.02
OUT	0.49 ±0.03	0.51 ±0.03	0.42 ±0.02	0.58 ±0.02	0.48 ±0.02	0.52 ±0.02
Day	0.49 ±0.03	0.51 ±0.03	0.39 ±0.01	0.61 ±0.01	0.52 ±0.02	0.48 ±0.02
Night	0.48 ±0.02	0.52 ±0.02	0.43 ±0.02	0.57 ±0.02	0.49 ±0.01	0.51 ±0.01
No Spill	0.50 ±0.01	0.50 ±0.01	0.43 ±0.01	0.57 ±0.01	0.49 ±0.01	0.51 ±0.01
Spill	0.36 ±0.03	0.64 ±0.03	0.39 ±0.02	0.61 ±0.02	0.52 ±0.02	0.48 ±0.02

Movement Fate Probabilities

The Markov-Chain analysis of fish movements resulted in estimates of the probability of passage out of particular sides of the sample volume. We call these "movement fates." For example, exit out the sluiceway side of the sample volume from the surface to 4 m deep corresponded to the "Sluice" fate. Possible fates were Sluice, Turbine, Bottom, East, West, Reservoir, and Not Moving. The data set included the region in front of the Sluice 1-2 entrance, 3.5-14.5 m upstream, and 5.5 m deep. The three-dimensional contour plot of the fate probabilities in Figures 19, 20, and 21 show 0.5 m slices +/- 3.5 on the centerline of Sluice 1-2 (X), 3.5-14.5 m from the dam (Y), and 1.0-5.5 m deep (Z). We present data for the sluice, bottom, and west fates because they are the most pertinent to this study.

The probability that fish exited the upper 4 m of the side of the Markov sample volume[4] facing the dam (the "sluice fate" probability) is instructive because it denotes passage toward the sluice entrance, one of two non-turbine passage routes at TDA. Based on visual inspection, the sluice fate probability pattern was similar, but not the same, with J-occlusions IN and OUT (Figure 19). The extent of noticeable sluice probabilities (> 0.2) was greater with the J-occlusions IN than OUT, extending out 10-12 m from the dam as opposed to 5-7 m (Figure 19). The extent of relatively high sluice probabilities during day resembled those during night with the J-occlusions IN, but was greater during night than day with J-occlusions OUT (Figure 19). Sluice probabilities were conspicuously lower during spill than no spill (Figure 19). Overall, the sluice probability contour plots showed that differences between J-occlusions IN and OUT were subtle and that spill negatively affected sluice fate probabilities.

The probability that fish exited the bottom of the Markov sample volume (6 m deep; "bottom fate" probability) is useful, because we would expect movement in that direction (presumably toward the turbine intakes) could be affected by the presence of the J-occlusions, which were located over the upper half of turbine intakes and formed a vertical barrier 7.6 m wide about 18 m deep. The bottom fate probabilities were similar between J-occlusions IN and OUT, between day and night, and between no spill and spill (Figure 20).

[4] Recall, the "Markov" sample volume was a subset of the total sample volumes for the two trackers and was identical for each J-occlusion condition.

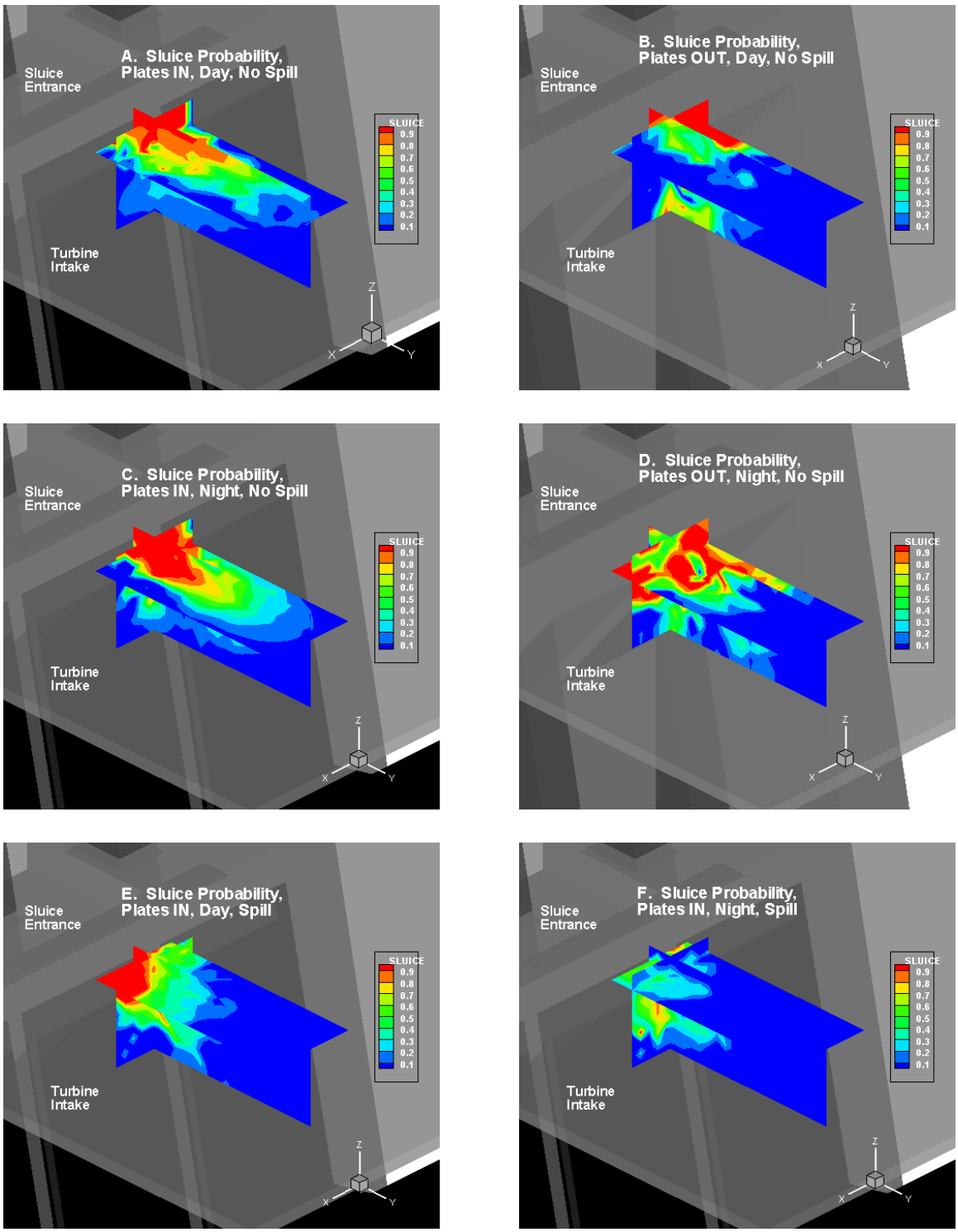

Figure 19. Sluice fate probabilities.

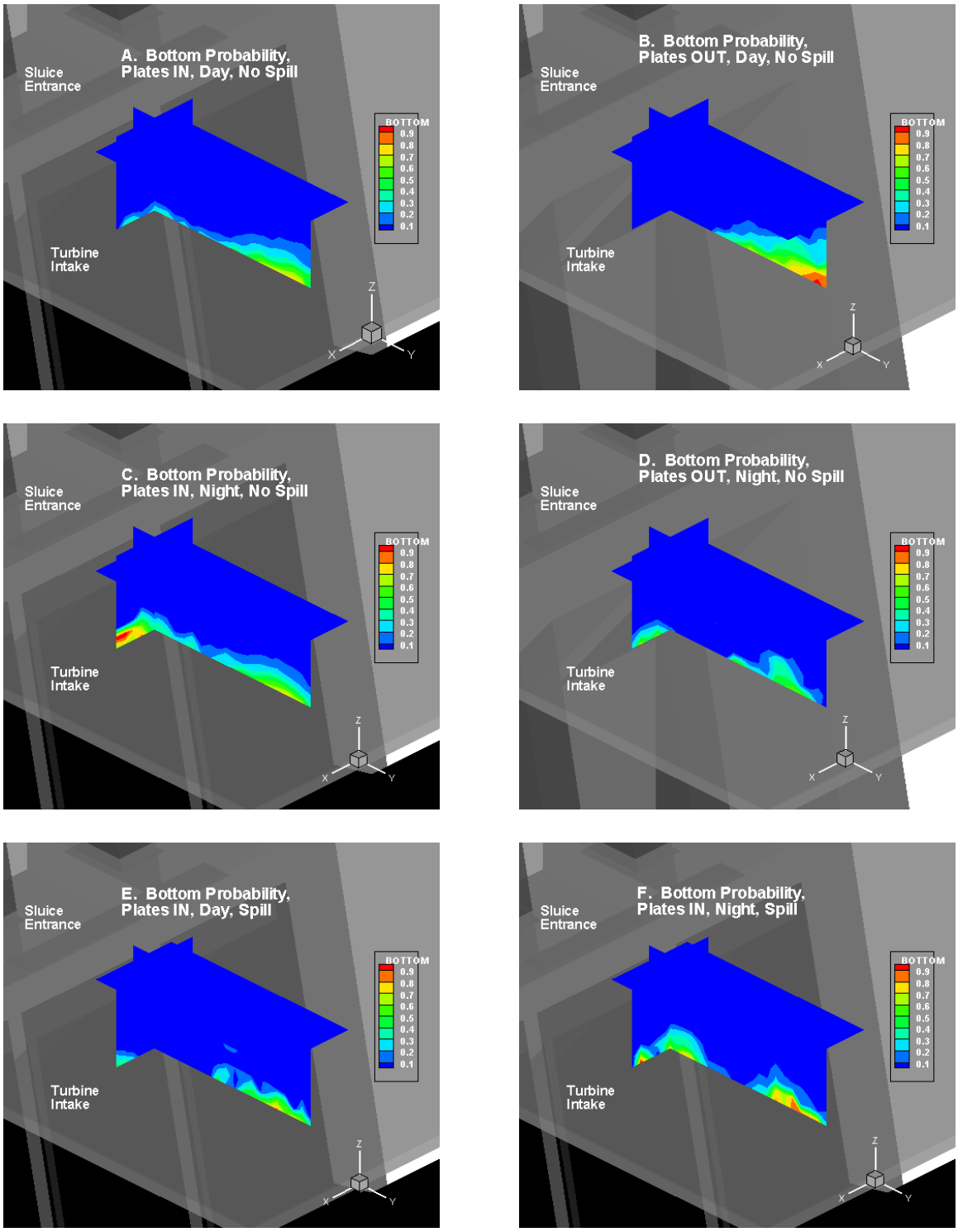

Figure 20. Bottom fate probabilities.

The probability fish exited the west side of the Markov sample volume ("west fate" probability) is important because movement westward toward the spillway due to the J-occlusions would be a positive effect if the fish otherwise would have passed into turbines. However, we did not observe much difference in the west fate between J-occlusions IN and OUT or between day and night (Figure 21). As expected from previous results, however, there was strong westward movement out of the sample volume during spill compared to no spill (Figure 21).

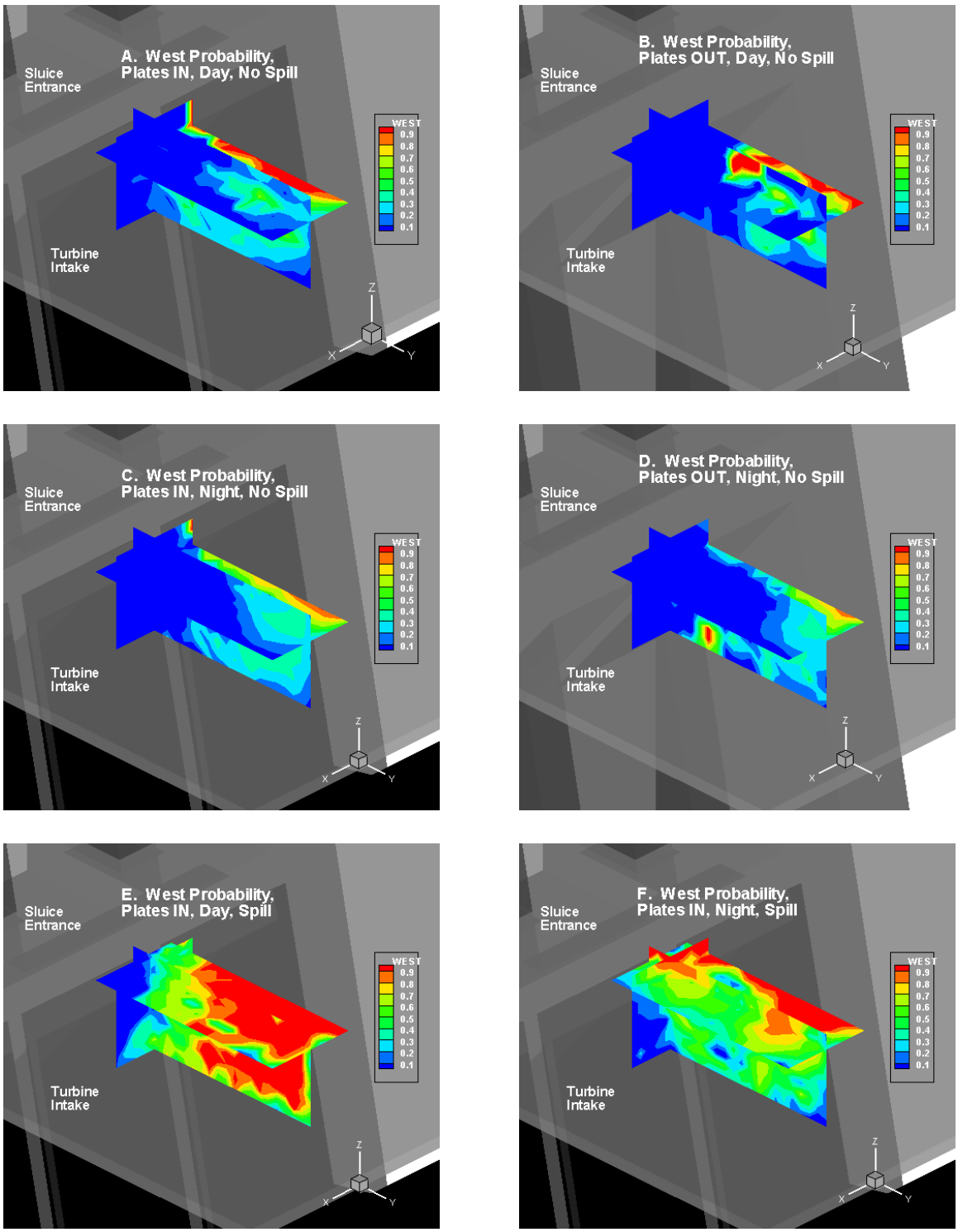

Figure 21. West fate probabilities.

Summary Analysis of Fate Probabilities

We summarized the fate probabilities by averaging the cell-by-cell data over the entire sample volume for fish tracked during no spillway discharge. (For the purpose of this analysis, the same sample volume was used for IN and OUT conditions.) The data presented in Figure 22 show:

- No prominent differences were observed between J-occlusions IN and OUT. The average difference between IN and OUT fate probabilities was less than 0.02 during day and less than 0.001 during night.
- East fate was the largest (0.33-0.36), followed by west (0.20-0.30) and sluice (0.21-0.30). The reservoir fate was the smallest (0.01-0.06).
- West fate was higher with J-occlusions IN than OUT (difference IN-OUT 0.03).
- Sluice fate was higher with J-occlusions IN during day (difference IN-OUT 0.02) but not during night (difference IN-OUT –0.05).
- Bottom fate was lower with J-occlusions IN during day (difference IN-OUT -0.02), but not during night (difference IN-OUT 0.02).

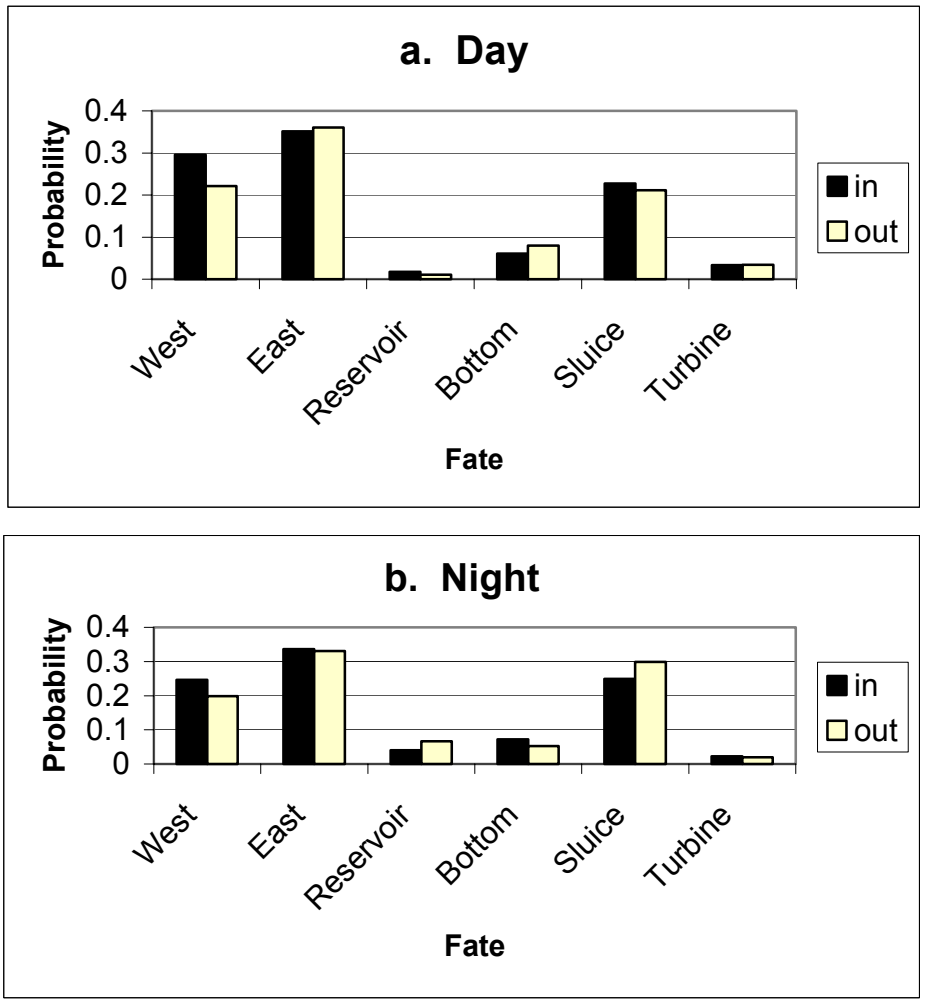

Figure 22. Mean fate probabilities from the Markov-Chain analysis for J-occlusions IN vs. OUT for day and night separately, no spill. (A similar plot for data collected during spill is not available because there were not enough data for the condition with J-occlusions OUT to run the Markov-Chain analysis.)

Assessment of Hypotheses about J-Occlusion Effects

In this section, we assess *a prioiri* hypotheses about the effects of the J-occlusions on smolt movements in the nearfield of Sluice 1-2. This assessment relies on volumetric analyses of fate probability data. It is qualitative, however, as there were no statistical comparisons.

Hypothesis -- The zone of influence for the sluiceway entrance at Sluice 1-2 will be larger with J-occlusions IN than OUT (as determined by fate probabilities).

Explanation – The flow net for the sluiceway, and hence its zone of influence, could be enhanced, or perceived to be such by smolts, due to less competing flow moving down toward the turbine intakes with J-occlusions in place.

Assessment – This hypothesis is not supported by the sluice fate volumetric data. If the zone of influence (ZOI) of the sluiceway is defined as the region where sluice fate probabilities are 0.9 or greater, then the sluice ZOI was smaller with J-occlusions IN (17 m^3 day and 27 m^3 night) than OUT (32 m^3 day and 48 m^3 night) (Figure 23).

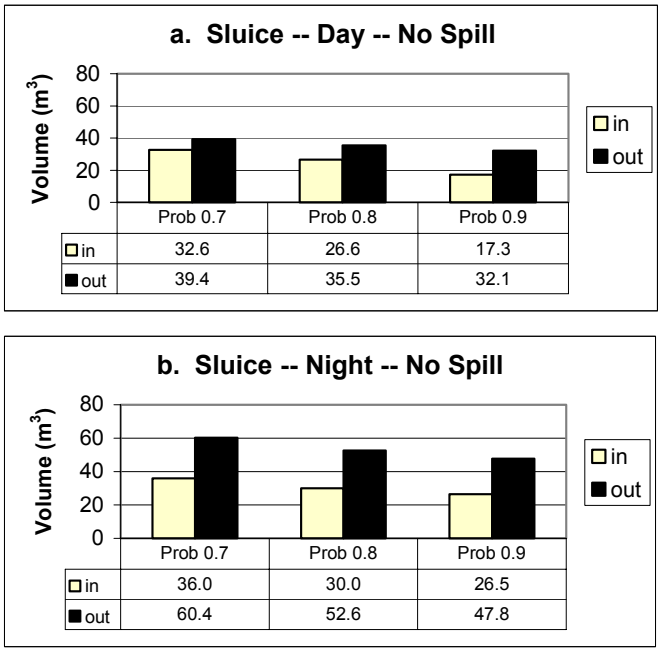

Figure 23. Volumetric analyses of sluice fate probabilities during no spill for day and night separately. The data are the total volume of cells in the Markov sample volume with sluice fate probabilities greater than 0.7, 0.8, and 0.9.

Hypothesis -- The overall probability of passage out the bottom of the sample volume toward the turbine intake will be lower with J-occlusions IN than OUT.

Explanation – Passage out the bottom of the sample volume might be less because the J-occlusions should decrease the downward flow toward turbines from the surface waters.

Assessment – This hypothesis is supported by the bottom fate volumetric data for day (Figure 24). For bottom fate probabilities greater than 0.9 during day, the volume was 2.4 m^3 with J-occlusions IN and 0.1 m^3 with them OUT. However, during night, there was no difference in bottom fates between J-occlusions IN and OUT (Figure 24) (2.5 vs. 2.6 m^3). In addition, the proportion of fish moving up in the water column (based on regression analysis) was greater with J-occlusions IN than OUT (52 vs. 50%, respectively) (Table 4).

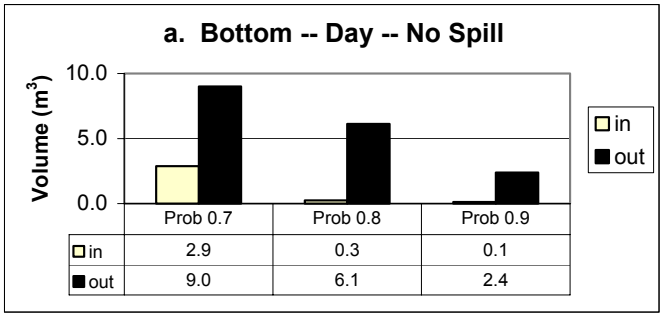

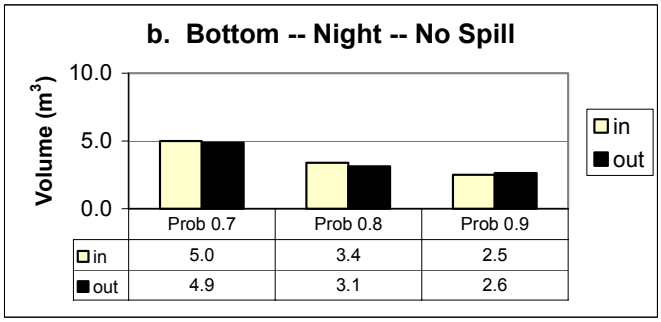

Figure 24. Volumetric analyses of bottom fate probabilities during no spill for day and night separately. The data are the total volume of cells in the sample volume with bottom fate probabilities greater than 0.7, 0.8, and 0.9.

Hypothesis -- The overall probability of passage to the west toward the spillway will be higher with J-occlusions IN than OUT during spill.

Explanation – The J-occlusions could serve to guide fish, which might otherwise pass into turbines, along the face of the dam to the west provided there is spill.

Assessment – Mean velocity in the X dimension was toward the west but had similar magnitude with J-occlusions IN and OUT (Figure 15). Thus, the available data do not indicate support for this hypothesis. (Markov-Chain analysis is not available because data for J-occlusions OUT during spill were too sparse.)

DISCUSSION

This study was designed to assess smolt movements in the nearfield (< 10 m) of the entrance to Sluice 1-2 and its associated turbine intake. The sample volume included the surface 6-8 m. It covered the 2-m region in front of the sluice sill as well as the top 2-4 m of the turbine intake below where the J-occlusions were installed/removed. Thus, the sample volume was directly applicable to study of J-occlusion effects on fish movements in front of Sluice 1-2 and the upper portion of Turbine Intake 1-2.

Effects of the J-occlusions on smolt movements can be assessed from two scales – large and small. Large-scale effects would be evident as noticeable, distinct differences in movement patterns between the IN and OUT conditions. On the other hand, small-scale effects would be subtle differences, including those that could perhaps even be masked depending on the analysis method. We did not observe large-scale effects due to the presence of the J-occlusions. Mean fish velocities, fish velocity streamtraces, movement proportions, and fate probabilities were all similar between J-occlusions IN and OUT. However, some small-scale differences were discovered that indicate positive effects of the J-occlusions.

Small-scale, but positive, effects of the J-occlusions were revealed in the mean fate probability and volumetric analyses. The mean probability of movement out the west side of the sample volume, toward the spillway, was 34% higher during day and 24% higher during night with J-occlusions IN than OUT. (Statistical significance was not assessed.) This indicates the J-occlusions may have resulted in guidance at the powerhouse toward the spillway, an encouraging development. The volumetric analysis showed many more cells had bottom fate probabilities greater than 0.7 with J-occlusions OUT than IN during day. This implies that the likelihood of fish movement downward, toward the turbine intake was less with the J-occlusions IN than when they were OUT, just as we would expect. This effect, however, was not observed during night, as IN and OUT bottom fate probability volumes were similar. The day/night differences in bottom fate suggest a possible visual effect from the J-occlusions. Therefore, there are some small-scale effects indicating indirectly that the J-occlusions may have been worthwhile.

While large-scale effects of the J-occlusions were not evident, such effects due to spill were noticeable. There was strong westward movement in the sample volume when water was spilled. This observation comports with previous data showing that

sluice passage efficiency and effectiveness decrease as the proportion of spill increases (Ploskey et al. 2001). Fish apparently guided along the face of the powerhouse and non-overflow section, following bulk flow toward the spillway. Thus, spill likely passed some fish that would otherwise have gone through the sluiceway. The important question is whether the J-occlusions guided fish to the spillway or sluiceway that would have otherwise passed in turbine. This question is unanswered at this time, although there are indications from our data this could have been the case, at least on a small-scale.

This study needs to be placed in the context of the comprehensive evaluation of fish passage using radio telemetry and fixed hydroacoustics at The Dalles Dam in 2001. While it is clear that the J-occlusions did not have a large-scale effect on fish movements in the nearfield of Sluice 1-2, some small-scale effects were observed. These effects may manifest themselves as indications of positive performance of the J-occlusions in the fish passage studies. In any event, further research is necessary in 2002 to assess whether J-occlusions are acceptable as a long-term smolt protection measure at The Dalles Dam.

CONCLUSIONS AND RECOMMENDATIONS

The conclusions that follow are based on the sonar tracker study of fish movements in the nearfield of Sluice 1-2 at The Dalles Dam in spring 2001.

1. In general, smolt movements were complex and multi-directional. Fish were not moving through the sample volume in a fixed, consistent direction.

2. Overall, the trend in movement regardless of treatment condition was westward (X-dimension; 56%), toward the dam (Y-dimension; 59%), and upward in the water column (Z-dimension; 51%).

3. Distinct differences between conditions with and without J-occlusions were not observed for mean fish velocity, streamtraces, direction of movement proportions, or movement fate probabilities.

4. The zone of influence of the sluiceway (region where Markov fate probabilities > 0.9) was almost half the size with J-occlusions IN than OUT.

5. The most noticeable factor affecting fish movements in the sample volume was spill. When water was spilled, the proportion of fish moving westward was 63% compared to 49% during no spill.

6. The J-occlusions seemingly did not positively affect fish movements in front of Sluice 1-2, because the J-occlusions did not increase movements toward the sluice entrance or enlarge the zone of influence at Sluice 1-2. This implies that any benefits of the J-occlusions will have to come from decreased turbine passage rates.

We have the following recommendations for research on fish movements associated with J-occlusions at The Dalles Dam in 2002.

1. Sample fish movement ~10 m further upstream and below the J-sections so that fish movement relative to the turbines can be assessed.

2. Sample fish movements with comparable intensities during all treatments with J-occlusions IN and OUT, so that the data sets can be reliably compared.

3. Sample fish moving toward turbines from mid water column, upstream of the J-occlusions.

4. Integrate fish movement and hydraulic data to explain fish responses to conditions created by the J-occlusions.

LITERATURE CITED

BioSonics, Inc. 1996. Hydroacoustic evaluation and studies at The Dalles Dam, spring/summer 1996. Volume 2 - Smolt behavior. Draft final report submitted to Portland District, U.S. Army Corps of Engineers by BioSonics, Inc. Seattle, WA. November 15, 1996.

BioSonics, Inc. 1998. DT/DE Series User's Manual Version 4.02. BioSonics, Inc., Seattle WA, 57 pp.

Brookner, E. 1998. Tracking and Kalman Filtering Made Easy. John Wiley and Sons, New York. 477 pp.

Dauble, D. D., S. M. Anglea, and G. E. Johnson. 1999. Surface flow bypass development in the Columbia and Snake Rivers and implications to Lower Granite Dam. Final Report submitted to Walla Walla District, U.S. Army Corps of Engineers by Battelle. Richland, WA. July 21, 1999.

ENSR, 2001. Three-Dimensional Computational Fluid Dynamics (CFD) Modeling of the Forebay of The Dalles Dam, Oregon. Final Report. June 2001. Document Number 3697-006-320. ENSR International, INCA Engineers. 206 pp.

Hedgepeth, J.B. and J. Condiotty. 1995. Radar tracking principles applied for acoustic fish detection. Poster Presentation, ICES International Symposium on Fisheries and Plankton Acoustics, Aberdeen Scotland, 12-16 June 1995, Book of Abstracts page 10.

Hedgepeth, J., D. Fuhriman and W. Acker. 1999. Fish behavior measured by a tracking radar-type acoustic transducer near hydroelectric dams. Pages 155-171 *in* M. Odeh, editor. Innovations in Fish Passage Technology. American Fisheries Society, Bethesda MD.

Hedgepeth, J.B., D. Fuhriman, G.M.W. Cronkite, Y. Xie and T.J. Mulligan. 2000. A tracking transducer for following fish at close range. Aquat. Living Resour. 13(5): 305-311.

Johnson, G. E. and A. E. Giorgi. 1999. Development of surface flow bypasses at Bonneville dam: a synthesis of data from 1995 to 1998 and a draft M&E plan for 2000. Final report ed. 1999 Oct 8.

Johnson, G. E. J.B. Hedgepeth, A. E. Giorgi and J.R. Skalski. 2001. Evaluation of smolt movements using an active fish tracking sonar at the sluiceway surface bypass, The Dalles Dam, 2000. Final report. September 30, 2001.

Johnson, R. L., D. R. Giest, R. P. Mueller, R. A. Moursund, J. Hedgepeth, D. Fuhriman, and A. Wirtz. 1998. Behavioral acoustic tracking system (BATS). Final report submitted to Walla Walla District, U.S. Army Corps of Engineers by Battelle. Richland, WA. January 1998.

Kumagai, K. K., Ransom, B. H., and Sloan, H. A. Effectiveness of a prototype surface flow attraction channel for passing juvenile salmon and steelhead trout at Wanapum Dam during summer 1996. Final report. Seattle, Washington: Hydroacoustic Technology, Inc. 1996.

MacLennan, D. N. and E. J. Simmonds. 1992. Fisheries Acoustics. Chapman and Hall. London, England. 325 pp.

Nagy, W. T. and M. K. Shutters. 1995. Hydroacoustic evaluation of surface collector prototypes at The Dalles Dam, 1995. Draft report by the Report by the Fisheries Field Unit, Portland District, U.S. Army Corps of Engineers. Cascade Locks, Oregon. 37 pages.

National Marine Fisheries Service 2001 B.O.

Nichols, D.W. and B.H. Ransom. 1980. Development of The Dalles Dam trash sluiceway as a downstream migrant bypass system for juvenile salmonids. Oregon Department of Fish and Wildlife. Report to U.S. Army Corps of Engineers, Portland, Oregon. Contract No. DACW57-78-C-0058. 36pp. + app.

Ploskey, G., T. Poe, A. Giorgi, and G. Johnson. 2001a. Synthesis of radio telemetry, hydroacoustic, and survival studies of juvenile salmon at The Dalles Dam (1982-2000). Final Report ed.; 2001 Sep.

Ploskey, G., B. Nagy, L. Lawrence, M. Hanks, C. Schilt, P. Johnson, G. Johnson, D. Patterson, and J. Skalski. 2001b. Hydroacoustic evaluation of juvenile salmon

passage at The Dalles Dam: 1999. Final report. ERDC/EL TR-01-11. Vicksburg, MS.

Ploskey, G., W. Nagy, L. Lawrence, D. Patterson, C. Schilt, P. Johnson, and J. Skalski. 2001c. Hydroacoustic evaluation of juvenile salmonid passage through experimental routes at Bonneville Dam in 1998. Final report. ERDC/EL TR-01-2. Vicksburg, MS.

Sokal, R.R and F.J. Rohlf. 1981. Biometry. The Principles and Practice of Statistics in Biological Research, 2 ed. W.H. Freeman and Company, San Francisco.

Taylor, H. and S. Karlin. 1998. An Introduction to Stochastic Modeling. 3rd ed. Academic Press. San Diego, CA. 631 pp.

Appendix A TECHNICAL DATA ON AFTS

In this appendix we present technical data on AFTS. Included are list of equipment, calibration data, echo sounder acquisition file, and tracker configuration data.

A.1 AFTS Equipment

The AFTS equipment we used in this study is listed in Table A.1.

Table A.1. List of AFTS equipment.

SERIAL NO.	DESCRIPTION
DT4000-96-036	DT echo sounder surface unit (208 kHz)
DT-Xmit-0165-04	DT underwater unit (“bottle”)
DT6-CH-200-6x15-007	Split-beam transducer, full beam width @ half-power (one-way) 6.6 degrees
141-95-946	Digital cable @ 100 ft
141-98-1239	Tracker cable @ 6 ft (bio p/n: 7000-2032)
#3	Tracker system, underwater unit with stepper motors and misc. cables
CPR-96-190	Tracker cables
N/a	Tracker motor control box, surface unit, with 50pF-50pF bus cable
2496-9103A	Dell Inspiron 7000
17971-98K-A6CH	DELL adapter
9078400043	LINKSYS Ethernet adapter
F3X171-10	BELKIN serial cable
Asset#2-300	Komodo monitor
M1055744	Keyboard

LTN60402395	Mouse
24X	24X MAX computer P166

A.2 Calibration Data

The acoustic calibration data for the split-beam system used in this study are presented in Table A.2.

Table A.2. Calibration data for AFTS's split-beam hydroacoustic system.

PARAMETER	VALUE
Receiver #1 Sensitivity @ 1 m	-123.40 dB_v || uPa
Receiver #2 Sensitivity @ 1 m	-126.75 dB_v || uPa
Source Level (Xmit = -6 dB)	219.39 dB_{uPa} @ 1 m

A.3 Echo Sounder Configuration

The following data are from the VISACQ.INI file that controls data acquisition with the DT4000 split-beam echo sounder system. Software version 4.02 was used.

- The SYSTEM section controls overall operation of the VISACQ program

  System

- Which drive to log data to

  FileDrive=C

- Begin running as soon as the program is started

  AutoRun=N

- Do we want to automatically save files

  AutoLog=N

- How are we limiting auto-named files: P for ping count, T for time (minutes) or S for size (kB)

LimitType=T

- What value for the limit: pings, minutes, or kB

  LimitValue=10

- Do we save the screen bitmaps (Y=save all bitmaps, 800 pings in each)

  SaveBitmaps=Y

- Which COM port has the GPS connected (-1 = not used)

  GpsPort=-1

- Main window placement - DO NOT CHANGE

  WindowPlacement=ffe9001003110254

- Default TVG for all views: 20 or 40 (default is 40)

  DefaultDisplayTVG=40

- Salinity of the water

  Salinity=0.0

- Temperature of the water

  Temperature=10.0

- Real Time Processing Configuration - how do we send the data?

  RTPUseTcpip=Yes

  RTPTcpipPort=2048

  RTPUsePrinter=Yes

  RTPPrinterPort=2049

  RTPPrinterChannel=1

  RTPUseSerial=No

  RTPSerialMode=BINARY

  RTPSerialPort=

  RTPSerialBaudRate=19200

  RTPTcpipTarget=90.0.0.1

RTPUseFile=No

RTPOutputFile=C:\DT4000.DTE

- The CHANNEL sections control the configuration of each transducer channel

  [Channel 1]

- Where does this window appear

  WindowPlacement=00160046021f01df

- Do we autorun this channel

  Run=Y

- Starting depth, in meters

  Start=1.0

- Stopping depth, in meters

  Stop=14.0 (also used 10.0 m about ½ time)

- Data threshold, in dB

  Threshold=-60.0

- Mode to threshold (0=FLAT, 1 = LINEAR, 2 = SQUARED)

  ThresholdMode=2

- Ping rate, in pings per second

  PingRate=30.0 (effectively only ~10 pps)

- Pulse width, in mSec

  PulseWidth=0.3

- Type of pulse (A=AMBIENT/NONE, C = CHIRP, M = MONOTONE)

  PulseType=M

- Do we want to use the timer functions for this channel (Y/N)

  UseTimer=N

- How long do we run for each burst

MinutesOn=20

- How long to stay off between bursts

  MinutesOff=10

- How long to "hold off" on start - initial delay time

  StartAfter=1

- Real Time processing configuration for this channel

  RTPOutput=No

  RTPBottomPeakThreshold=-35.0

  RTPBottomPeakWidth=0.10

  RTPBottomBlankingThreshold=-60.0

  RTPBottomBlankingZone=0.25

  RTPBottomBottomWindow=1.50

  RTPBottomUsePreset=YES

  RTPBottomPresetDepth=60.0

  RTPTrackingCorrelation=0.90

  RTPMinTrackingEchoStrength=-70.0

  RTPMaxTrackingEchoStrength=-30.0

  RTPMinTrackingRange=1.00

  RTPMaxTrackingRange=60.00

  RTPMinTrackingEchoWidth=0.80

  RTPMaxTrackingEchoWidth=1.20

  RTPMinTrackingAlongshipAngle=-6.0

  RTPMaxTrackingAlongshipAngle=6.0

  RTPMinTrackingAthwartshipAngle=-6.0

  RTPMaxTrackingAthwartshipAngle=6.0

  RTPMinDualBeamTrackingEchoDifference=0.0

RTPMaxDualBeamTrackingEchoDifference=6.0

RTPMaxTrackingEchoes=25

- Tracker

  Output=Y

  Channel=1

  Start=1.0

  Stop=20.0

  Threshold=-60

  ComPort=1

  MinTargetRatio=0.5

  MaxTargetRatio=3.5

  TimerDuration=30

  PassiveMode=N

A.4 Tracker Configuration

The tracker configuration was contained in a file called TSS1.CFG. This file is printed below.

- MAIN MISC.

  maximum ping rate [real, pings/sec] = 10 /{R}

  max lines in file [int] = 10000 /{R}

  display graphs [Y/N] = Y /{W,N}

  graph scales equal [Y/N] = Y /{DW,Y}

- POSITIONING MISC

  key move angle [real, degrees] = 5.0 /{R}

  allow angle error [real, degrees] = 2.0 /{R}

  install alpha [real, degrees] = 10.0 /{R}

  alpha margin [real, degrees] = 2.0 /{R}

beta margin [real, degrees] = 2.0 /{R}

auto position check [Y/N] = Y /{R}

minutes between position checks [real, minutes] = 30.0 /{DW,20}

max idle time minutes [real, minutes] = 0.10 /{R}

free track time minutes [real, minutes] = 2.0 /{R}

reset idle pings/track threshold [integer] = 5 /{W,5}

- POSITIONING OPTIONS -- RANDOM START POSITION

  random start position [Y/N] = Y /{R}

  pos radius min [real, meters] = 1.0 /{DR}

  pos radius max [real, meters] = 14.0 /{DR}

  pos alpha min [real, degrees] = 30.0 /{DR}

  pos alpha max [real, degrees] = 95.0 /{DR}

  pos beta min [real, degrees] = -5.0 /{DR}

  pos beta max [real, degrees] = 52.0 /{DR}

- POSITIONING OPTIONS -- SPECIFIC START POSITION

  specific start position [Y/N] = N /{W,N}

  start alpha angle [real, degrees] = 30 /{DR}

  start beta angle [real, degrees] = -6 /{DR}

- SPECIAL CONTROL 1

  special control 1 [Y/N] = Y /{W,N}

  range gate width [real, meters] = 20 /{DR}

  range gate middle [real, meters] = 10 /{DR}

  range width change increment [real, meters] = 1.0 /{DW,2.0}

  range middle change increment [real, meters] = 1.0 /{DW,2.0}

  max reacquire distance [real, meters] = 3 /{DR}

max reacquire pings [integer] = 20 /{DR}

range gate angle width (+/-) [real, degrees] = 3 /{DR}

- MOTOR CONTROL

  motor settle delay seconds [real, seconds] = 0.02 /{W,0.02}

  motor speed number [integer] = 2 /{W,2}

  range step error [integer] = 3 /{W,3}

- TELEGRAM RECEIVING

  com port [1/2] = 1 /{R}

  com rate [integer, bps] = 115200 /{W,115200}

- COORDINATE ROTATION

  rotate coordinates [Y/N] = N /{W,N}

  lock coordinates [Y/N] = Y /{DW,Y}

  Cxx [real] = 1 /{DR}

  Cxy [real] = 0 /{DR}

  Cxz [real] = 0 /{DR}

  Cyx [real] = 0 /{DR}

  Cyy [real] = 1 /{DR}

  Cyz [real] = 0 /{DR}

  Czx [real] = 0 /{DR}

  Czy [real] = 0 /{DR}

  Czz [real] = 1 /{DR}

- TRANSDUCER -- STANDARD TS COMPENSATION

  beam angle [real, degrees] = 6.6 /{DR}

- TRANSDUCER -- SPLIT-BEAM ANGLES

  phase aperture [real, degrees] = 6.8 /{DR}

invert angle sign [Y/N] = Y /{DR}

along offset [real, degrees] = 2 /{W,0}

athwart offset [real, degrees] = 2 /{W,0}

- TRANSDUCER -- PARALLAX CORRECTION

  soft PC [Y/N] = Y /{R}

  space along [real, meters] = 0.039 /{DR}

  space athwart [real, meters] = 0.039 /{DR}

  approx. for 208k: space along = 0.03735, space athwart = 0.03735

  approx. for 201k: space along = 0.03839, space athwart = 0.03839

  approx. for 430k-6x5: space along = 0.0185, space athwart = 0.0185

- TRACKING

  track error beep [Y/N] = N /{W,N}

  continue track with errors [Y/N] = N /{W,Y}

  max pings in track [integer] = 799 /{W,799}

  max pings in error track [integer] = 1200 /{W,1200}

  max speed [real, meters/sec] = 4.0 /{R}

  min dist mult [real] = 3.0 /{R}

  max delta time [real, seconds] = 0.5 /{W,1.0}

- PREDICTIVE TRACKING

  predictive tracking [Y/N] = Y /{R}

  weight 1 = 1.0

  weight 2 = 0.5

  weight 3 = 0.25

  weight 4 = 0.125

- TARGETING BOUNDARIES

compTS low [real, dB] = -60 /{R}

compTS high [real, dB] = -10.0 /{R}

target radius min [real, meters] = 1.00 /{R}

target radius max [real, meters] = 17.0 /{R}

target x min [real, meters] = -5 /{R}

target x max [real, meters] = 20 /{R}

target y min [real, meters] = -2 /{R}

target y max [real, meters] = 20 /{R}

target z min [real, meters] = 0 /{R}

target z max [real, meters] = 9.0 /{R}

- TRACKING BOUNDARIES (no compTS check for tracking)

  tracking use target bounds [Y/N] = N /{W,Y}

  track radius min [real, meters] = 1.0 /{DR}

  track radius max [real, meters] = 20.0 /{DR}

  track x min [real, meters] = -10 /{DR}

  track x max [real, meters] = 25 /{DR}

  track y min [real, meters] = -2 /{DR}

  track y max [real, meters] = 25 /{DR}

  track z min [real, meters] = -10 /{DR}

  track z max [real, meters] = 9 /{DR}

- ADDITIONAL TRACKING BOUNDARIES

  track alpha min [real, degrees] = -72 /{R}

  track alpha max [real, degrees] = 95 /{R}

  track beta min [real, degrees] = -62.0 /{R}

  track beta max [real, degrees] = 52.0 /{R}

- SAVED DATA FILTER BOUNDARIES

  saved data filter [Y/N] = N /{W,N}

  saved use tracking bounds [Y/N] = Y /{DW,Y}

  save radius min [real, meters] = 1 /{DR}

  save radius max [real, meters] = 50 /{DR}

  save x min [real, meters] = -50 /{DR}

  save x max [real, meters] = 50 /{DR}

  save y min [real, meters] = -50 /{DR}

  save y max [real, meters] = 50 /{DR}

  save z min [real, meters] = -50 /{DR}

  save z max [real, meters] = 50 /{DR}

  save alpha min [real, degrees] = -100 /{DR}

  save alpha max [real, degrees] = 100 /{DR}

  save beta min [real, degrees] = -55 /{DR}

  save beta max [real, degrees] = 55 /{DR}

APPENDIX B TRACKING DETAILS, AFTS

The Active Fish Tracking Sonar (AFTS) uses four angles, plus range, to track a fish target (Figure B.1). Two are angles from a split-beam transducer to the fish. Another two angles are from two rotator motors, which are required to drive the transducer to point directly at the fish target. These four angles plus range to the fish target enable a fish position to be estimated in terms of a Cartesian coordinate system: x, y and z.

The BioSonics DT6000 split-beam echosounder (DT) uses a unique configuration (Figure B.1). The split-beam transducer angles are measured from three circular piezo-electric ceramics in the transducer: center, x and y. A fourth, larger, circular ceramic in the transducer transmits the sound pulses, which are reflected from a fish and used by the angle-measuring elements. The reflection into the large ceramic is used to determine the range to the fish target (and also for measuring sound intensity for target acquisition and acoustic size estimation).

Rotator Angles

The outer armature is driver by a stepper motor which half steps (0.9 degrees per half step) but is geared by a factor of ten, which suggests the angle resolution is 0.09 degrees, but, due to backlash, has a total possible error of about +/- 0.2 degrees. The inner armature is geared by a factor of 4.8 and, with backlash, has a possible error of about +/- 0.3 degrees.

Split-beam Angles

The two split-beam transducer angles, γ and ψ, are used directly to measure relative Cartesian coordinates of the fish after measuring range R to the fish, i.e.:

$$x' = R\,\sin(\gamma)$$
$$y' = R\sin(\psi)$$
$$z' = R^2 - x'^2 - y'^2$$

The design of the BioSonics transducer requires that planar angles be translated by a parallax correction described below, discussed in Johnson et al. (2001). This translation assumes that the split beam angles are made in planes orthogonal to each other. However, the geometry is not necessarily at right angles to the main beam axis, (Figure B.2) (W.T. Nagy, pers. comm.). Nagy refers to the split-beam angles as conical angles, as the volume swept by a fixed angle describes a cone. Slight errors unreported

in Johnson et al. (2001) can occur, especially when the fish is at closet range and at 45 degrees to the split beam pairs. In consequence, we recommend translating the split beam angles into angles in planes orthogonal to one another before the parallax correction is made. The two orthogonal angles (intersecting at the beam axis) are

$$lambda1 = atan(x'/z)$$
$$lambda2 = atan(y'/z').$$

It would be simple to correct for parallax, or to use these angles for tracking. During this study we assumed that the split-beam angles were orthogonal for parallax correction, but we used the conical angle solution for coordinates. Given the solution for orthogonal angles (above) it would be relatively simple to transpose to the main element, to correct parallax. Solving for the planar angles should be an improvement to the tracker. In addition, it is then consistent for the beam factor B solution for the standard split-beam:

$$B = \alpha\, lambda1^2 + \beta\, lambda2^2$$

where, B is based on the orthogonal geometry. However, the orthogonal geometry is NOT assumed in the tracking equations discussed below.

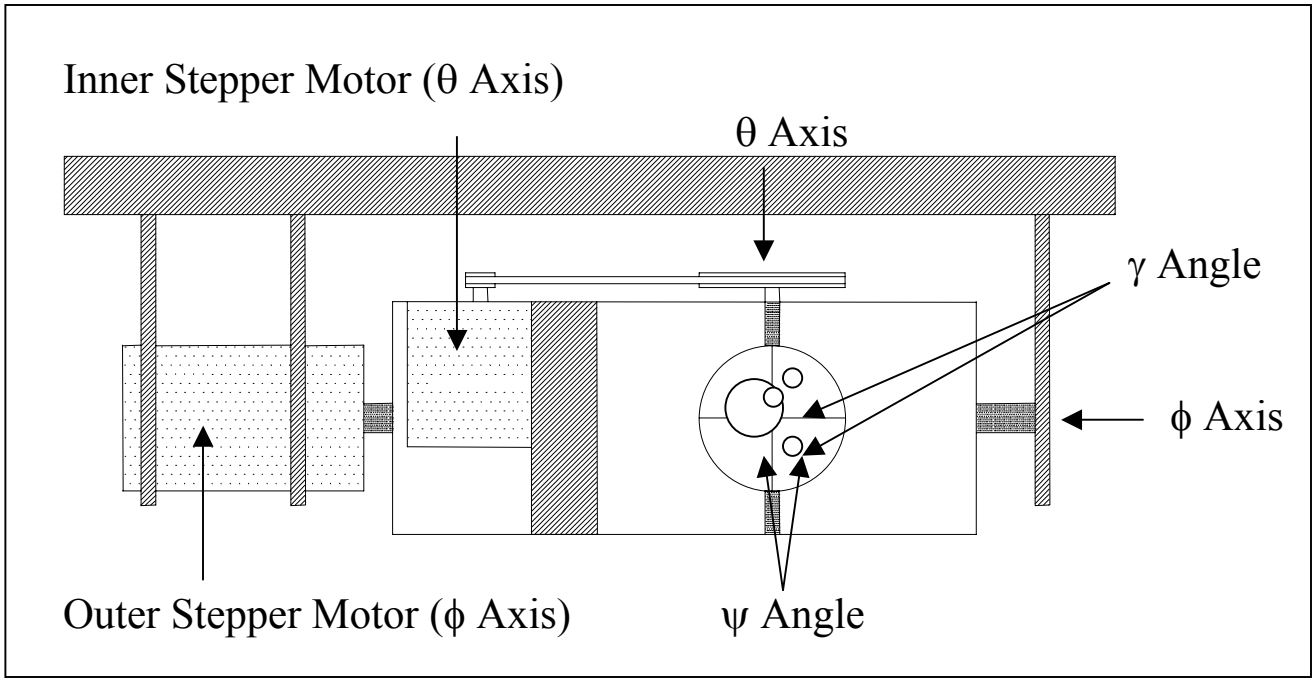

Figure B.1. Photo and diagram of the Acoustic Fish Tracking Sonar (AFTS). The angles to target position from a split beam transducer are measured using two piezo-electric ceramic receivers for comparisons of phase. Once the angles (□.□) from the fish reflection are determined, they are used to determine new rotator motor angles (□.□) towards the target. Motors turn the transducer to follow fish movement.

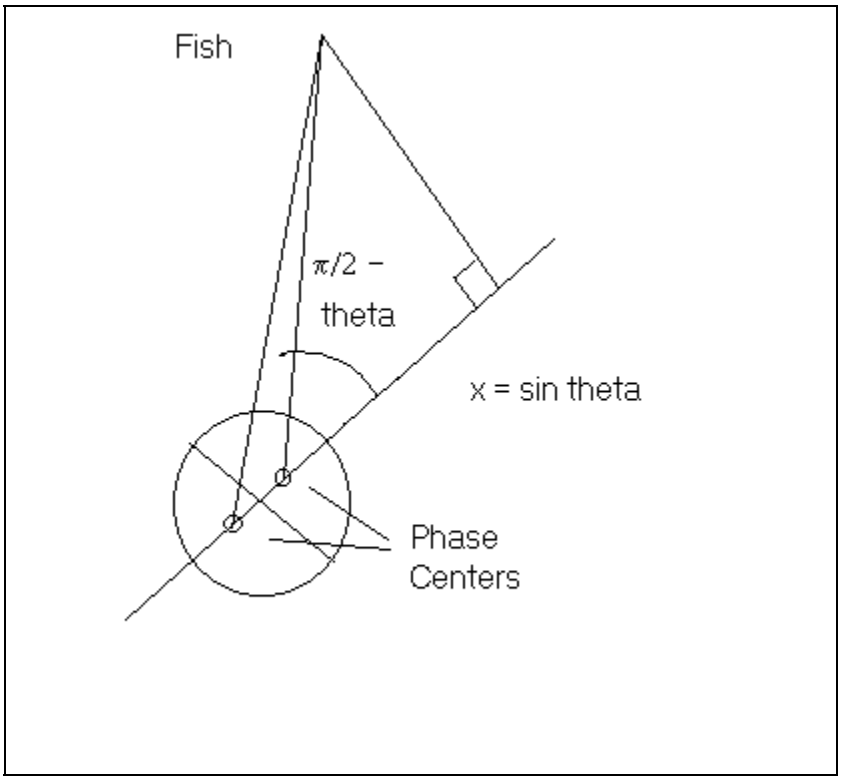

Figure B.2. A split-beam angle theta (the complement describing fish to line in transducer plane) is used to compute Cartesian coordinate x', where range is assumed to be 1.

Quadrature Components

The phase differences between a pair of receivers gives us one planar angle to the fish target. Quadrature sampling is one way to estimate phase difference. If the signal *S(t)* from one of the receivers can be expressed as

$$\begin{aligned} S(t) &= A(t)\cos[\omega_0 t + \varphi(t) + \theta] \\ &= X(t)\cos(\omega_0 t) + Y(t)\sin(\omega_0 t) \end{aligned}$$

The quadrature components *X(t)*, *Y(t)* are the samples one quarter of a wavelength apart

$$\begin{aligned} X(t) &= A(t)\cos[\varphi(t) + \theta] \\ Y(t) &= -A(t)\sin[\varphi(t) + \theta] \end{aligned}$$

where θ = arbitrary angle offset

$\varphi(t)$ = phase

$A(t)$ = amplitude

$\omega(t)$ = carrier frequency of signal

The phase of one receiver is estimated by

$$\varphi(t) = \tan^{-1}\left(\frac{-Y(t)}{X(t)}\right)$$

By repeating this process on two receivers, a phase difference can be calculated. This phase difference $\Delta\varphi(t)$ can only be measured only in the range of plus or minus π radians. It is referenced to the wavelength of the carrier frequency $\omega(t)$ measured in radians s-1.

The next step is to covert the phase difference to an actual angle $\theta(L)$ to the fish target. The phase aperture is the maximum physical angle that can be determined from the electrical phase output, compared between two ceramics separated at distance D between acoustic centers. This angle occurs at phase wrap, and is equal to plus or minus arcsine(wavelength/distance between receivers). The wavelength □ is equal to the sound speed c times the frequency f in cycles s-1. $\theta(L)$ can be calculated using a small angle approximation

$$\theta(L) = \sin^{-1}\left(\frac{c\ \Delta\varphi(t)}{2 f D \pi}\right)$$
$$\cong \frac{c\ \Delta\varphi(t)}{2 f D \pi}$$

and the phase aperture is the maximum angle before phase wrap occurs, and using the small angle approximation is

$$\pm \frac{c}{2 f D}.$$

The spacing between the elements for estimating phase difference in the BioSonics 208 kHz split-beam transducer was 0.03018 m. The phase aperture is +/-6.77 degrees letting the speed of sound c be 1480 m/s.

Parallax is an error that is encountered because of the difference in location of the main beam ceramic and the pair of ceramics that estimate a planar angle. The parallax correction is performed in the tracking software, and affects the estimated target strength primarily. The parallax to the armature center may introduce another slight error in angle for tracking a fish target. The spacing D' between acoustic centers of the main beam ceramic and the pair measuring angle was measured as 0.03735 m for the 208 kHz transducer. The parallax correction is dependent on range R to the tracked fish, and is:

$$\gamma' = \gamma - \sin^{-1}\left(\frac{\mathrm{D}'\cos\gamma}{R}\right).$$

Target Tracking

The operation of AFTS involves two sets of angles: those of the stepper motors and those of the split-beam transducer. To accomplish fish tracking, the split-beam phase angles, γ and ψ needed to be compensated by the stepper motor angles θ and ϕ (Figure II.1).

The following analysis shows the fundamental equations for rotation; it assumes a dam-referenced coordinate system (x, y, z). The x-axis runs along the dam to the right when facing away from the dam, the y-axis points up, and the z-axis points away from the dam. Let the unit vectors in the absolute coordinate system be $\hat{i}$, $\hat{j}$, and $\hat{k}$. Then unit vectors of the rotated coordinate system (ξ,η, and ζ) of the transducer are:

$$e_\xi = \cos\theta\,\hat{i} - \sin\theta\sin\phi\,\hat{j} - \sin\theta\cos\phi\,\hat{k}$$
$$e_\eta = \qquad\qquad \cos\phi\,\hat{j} - \qquad \sin\phi\,\hat{k}$$
$$e_\zeta = \sin\theta\,\hat{i} + \cos\theta\sin\phi\,\hat{j} + \cos\theta\cos\phi\,\hat{k}$$

The unit vector to a fish target is:

$$e_\rho = \sin\psi\, e_\xi - \sin\gamma\, e_\eta - \sqrt{1-\sin^2\gamma\ -\sin^2\psi}\, e_\zeta$$

In terms of the stepper motor coordinate system the unit vector to the fish is:

$$\begin{aligned} e_\rho \quad &= \left(\cos\theta\sin\psi \ +\sin\theta\sqrt{1-\sin^2\gamma\ -\sin^2\psi}\right)\hat{i} \\ &+\left(-\sin\theta\sin\phi\ \sin\psi\ +\cos\phi\ \sin\gamma\ +\cos\theta\sin\phi\sqrt{1-\sin^2\gamma\ -\sin^2\psi}\right)\hat{j} \\ &+\left(-\sin\theta\cos\phi\ \sin\psi\ -\sin\phi\ \sin\gamma\ +\cos\theta\cos\phi\sqrt{1-\sin^2\gamma\ -\sin^2\psi}\right)\hat{k} \end{aligned}$$

The new stepper motor angles required to follow the fish are:

$$\theta' = \sin^{-1}\left(\cos\theta\sin\psi \ +\sin\theta\sqrt{1-\sin^2\gamma\ -\sin^2\psi}\right)$$

$$\phi' = \tan^{-1}\left(\frac{-\sin\theta\sin\phi\ \sin\psi\ +\cos\phi\ \sin\gamma\ +\cos\theta\sin\phi\sqrt{1-\sin^2\gamma\ -\sin^2\psi}}{-\sin\theta\cos\phi\ \sin\psi\ -\sin\phi\ \sin\gamma\ +\cos\theta\cos\phi\sqrt{1-\sin^2\gamma\ -\sin^2\psi}}\right)$$

In addition to these two equations for following fish, we have attempted to predict where the fish moves, and rotate the beam axis towards that position. An algorithm predicted incremental movement in Δx, Δy and Δz separately using the following equation (shown for Δx):

$$\Delta x = \frac{\left(x_i - x_{i-1}\right) + 0.5\left(x_{i-1} - x_{i-2}\right) + 0.25\left(x_{i-2} - x_{i-3}\right) + 0.125\left(x_{i-3} - x_{i-4}\right)}{1.875}$$

Our predictive method is an “ad hoc” implementation of a discounted least-squares fit (Brookner 1998) in which the most recent velocity estimate is weighted by unity, the next most by ω=0.25, the next oldest by ω^2, the next by ω^3 and so on. In our “ad hoc” implementation we stop at ω^3 and assume that time between pings is constant.

APPENDIX C: COMMENTS ON DRAFT FINAL REPORT

Comments on the draft final report dated October 31, 2001 were received from Dr. Cliff Pereira, Oregon State University. His memorandum is reproduced below. Our responses to his comments are inserted in the text.

January 14, 2001
TO: Blaine Ebberts
FROM: Cliff Pereira
RE: Comments on the draft final report: Sonar tracker evaluation of fish movements relative to J-Occlusions at The Dalles Dam in 2001 by Hedgepeth, et al.

The basic approach is reasonable given that the J-occlusions could not be moved as planned in the experimental design.

Page 10. Figure 8. If there is interest in being able to resolve the profiles for stocks with smaller runs, then a change in this graph is needed. One way to see them all is to change to a log style axis for Smolt Passage Index. If it is thought that a log style would be difficult for the reader to interpret, then another choice would be to have a second graph that only goes from zero to about 10,000. However, I believe that most people can interpret a log style axis.

> Agree. The axis of the figure was transformed to a logarithmic (base 10) scale.

Page 11. The predictive tracking algorithm sounds interesting. How do we know that there is not a selectivity to the tracker? That is would it be possible that fish that are changing direction only a little would have a higher probability of being detected compared to fish that are changing direction quite a bit?

> Detection is a function of signal-to-noise in the acoustic tracking process. Our acoustic system used a low threshold, and thus tracked small targets reasonably well. Fish directivity (signal strength) changed as a function of aspect, and therefore tracking may be differentially successful in different parts of the volume surveyed. Once a fish was detected and tracking was initiated, success in following a fish also depended on the quality of the tracking algorithm. We used the predictive algorithm to adapt to fish that changed direction "quite a bit" to minimize any "selectivity." It would be possible to investigate the use of other types of tracking algorithms to see if improvements could be made. A distribution of tracked fish speeds in a particular slice of the water volume might also shed light about tracking selectivity. We expect that it is harder to track fish very close to the transducer (for example one meter range) because the volume sampled by the acoustic beam is small there.

Page 13. The authors state that sample deployments and sample volumes differ between treatments. How do we know that at least some of the differences one might see between treatments could be attributed to deployment and sample volume differences.

> The treatment comparison used the same sample volumes for each, i.e., subset volumes were identified where the two different samples volumes for J-occlusions IN and OUT overlapped.

Page 15. Table 2 shows the number of tracks per day. Note that approximately 26 of the 32 days have over 500 tracks per day and there is never fewer than 150 tracks in a day. This suggests that many graphics and analyses can be done on a daily basis to show day to day variation which after all is the basic unit of this study. (They are studying day and night studies and there are discrete day periods every 24 hours, making them the natural units for analysis. These daily results can be used to better look for transitions and show transitions (such as the no-spill to spill transition. The daily data can also be used to assess assumptions such as independence or stationarity used in the Markov Chain analysis.

> Mostly disagree. Daily data probably could be used to estimate mean velocities and overall movement proportions, but would be insufficient (too few data points) be used for analyses showing spatial trends from cell to cell, e.g., streamtraces and Markov probabilities. We combined data over study-days to address the primary objective to compare fish movement patterns with and without J-occlusions.

Page 19. Bottom. The fish track directionality regressions need more explanation. Rather than attempt to explain it completely, it might make more sense to show several small examples. These should include example fish tracks where the results of the regressions will clearly differ from the simplistic process of simply taking the direction formed from just using the first position and the last position of the track. That is, the examples should show why one should do these regressions rather than simply connect the first and last positions to get a direction.

> Agree. The regression explanation was reworded and a figure was added.

Page 20. It is good that the authors mention assumptions of the Markov-chain analysis. It is clear that the first assumption is assessed, but is there an attempt to assess the second and third assumptions (independence and stationarity)? I may have missed it. Can one take samples of cells and see how the probability estimates (proportions in the middle of page 21) change from day to day (since days are natural units here). It would seem that they can assess whether or not the variation in these daily observed proportions is consistent with the independence and stationarity assumptions.

> Agree, but we do not have a sufficient number of tracked fish on a daily basis to perform an analysis by day over a period of several days [[**JBH? Let's do it??]]** it would shed light about the stationarity of our results over day lags. A way of looking at the stationarity assumption in our Markov-Chain analysis would be to vary the time step (we used one second) and see if the results are similar. Such a test was not performed in our analysis **[[JBH?? Do it??]].** It is reasonable to assume independence because we sampled the volume randomly and uniformly.

Page 22. It is excellent that the authors check the first assumption (Markov property). It is not clear what is meant by "As many cells as were practical were tested in this manner." Does this mean that they simply ran out of time or money to do more than 496 (which is quite a few) out of the possible 726, or were some cells more problematic and in some sense "not practical" to test.

> Cells where the number of fish positions was greater than 10 were tested in this manner. This point was added to the text.

The authors claim that because the null hypothesis was rejected in fewer than 9% , "this is a good indication that our use of the Markov chain was appropriate …" If indeed the

null hypothesis is true throughout, then the expected percent of rejections is 5%. Therefore it is important to ask if the observed 42 out of 496 (8.46%) is reasonably consistent with the expected 5% (i.e., is the difference attributable to chance?) It is not clear from the description of these tests whether or not they can be treated as independent. (An example or two would be nice to make it clear what they are doing.) If it is reasonable to treat the tests as independent, then an exact binomial test can be used to assess the question. Since we are interested in more rejections than expected a one-sided test would be appropriate here. The exact one-sided p-value is 0.0007 which is strong evidence that the null model does not fit the results. That is, with an N of 496 independent tests, 8.46% rejecting is significantly greater than expected under the null of a 5% rate (p=0.0007 exact binomial test). So the authors need to (1) discuss the independence of the tests and (2) if reasonable to assume independence, then they need to report rejection of the null hypothesis and its implication for the use of the Markov chain.

> Tests were conducted on individual spatial cells. For each individual cell, counts were tallied for cell combinations from which and to which fish moved. Because as much data as possible were used, it is conceivable that one fish could have supplied more than one count in a contingency test, and also one fish could be represented in more than one contingency test (when movement took place through more than three cells). However the first case would be rare and the second case should not violate the independence requirement for an individual test. These fish were randomly sampled, in that the water volume was randomly surveyed. In consequence, we assume independent sampling for fish.
>
> It is true that 8.46% is significantly different than 5% with n = 496. In addition, it is not significantly different than 10%. The 95% confidence limits are approximately 6% to 12%. We can be reasonably certain that fewer than 12% of the cases would violate the Markov assumption of history independence, but that at least 6% would violate that assumption. Thus our data are significantly better than those with say 25% of rejections of previous movement independence. Thus we feel able to justify using the Markov transition matrix approach.

Page 33 and 39 Figures 18 to 20 and Figure 22. It is noted that in figure 18 the "extent of noticeable sluice probabilities (>0.2) was greater with the J-occlusions IN than OUT." On Page 38 it is noted that the volume with probability greater than 0.9, 0.8 and 0.7 (in figure 22) is smaller with the J-occlusions IN than OUT. The authors need to help the reader see why these change direction between Figure 18 and figure 22. Should these two figures comport? What is happening at probabilities between 0.6 and 0.2 that make the first statement the way it is compared to the second. Or are they talking about very different things that should not comport.?

> Figures 18-20 are descriptive, whereas Figure 22 is quantitative. They do not necessarily have to comport as they are used to make different points, one dealing with qualitative "extent" and the other with quantitative "volume."

Page 43. It is stated that "Overall, the trend in movement was …. Upward in the water column (Z-dimension); 51%). It would seem more appropriate to say that about half were going up and half were going down rather than that the trend was upward when only 51% are going upward.

> Agreed. This part of the text was completely rewritten.